JPRS-UEQ-90-007
7 MAY 1990

FOREIGN BROADCAST INFORMATION SERVICE

JPRS Report

Science & Technology

USSR: Engineering & Equipment

JPRS-UEQ-90-007
7 MAY 1990

SCIENCE & TECHNOLOGY

USSR: ENGINEERING & EQUIPMENT

CONTENTS

INDUSTRIAL TECHNOLOGY, PLANNING, PRODUCTIVITY

UDC 535.32:681.785.55

Optical System With Increased Dispersion

907F0200A Baku DOKLADY AKADEMII NAUK AZERBAYDZHANSKOY SSR in Russian Vol 45, No 5, May 89 (manuscript received 29 Jan 88) pp 24-27

[Article by T. G. Dilbazov and N. F. Mirzoyeva, Scientific Production Association of Space Research]

[Text] The development of various fields of science and technology has led to a new phase of spectral instrument building. New methods of spectroscopy are being developed, and high-quality spectral instruments that permit various types of research work have been created [1]. Despite the enormous capabilities of these instruments, classical instruments with one-dimensional dispersion remain primary in fundamental and applied research. Therefore, one of the directions of all optical instrument building is to improve the characteristics of optical systems.

The results of research, devoted to improving one of the main parameters of an optimal system--dispersion, are presented in this paper.

Existing methods of increasing the dispersion of optical systems [2-5] are hardly effective and are ordinarily related to complication of the optical system, which results in intensification of absorption and aberrations of the system.

The linear dispersion of an optical system is determined by the formula

$$D = \frac{dl}{d\lambda} = f_2 \frac{d\varphi}{d\lambda}, \qquad (1)$$

where dl and $d\varphi$ are the linear and angular distance between spectral lines with wavelength λ and $\lambda + d\lambda$ in the focal plane and f_2 is the focal distance of the camera objective.

It is obvious from (1) that linear dispersion can be increased by two methods: 1) by an increase of the focal distance of the camera objective. This method is used frequently in development of spectral

instruments with large dispersion, but always results in an increase of the overall dimensions of the instrument; and 2) by an increase of the angular dispersion of the system. Angular dispersion for instruments with a prism is limited by the dimensions and material of the prism. An increase of angular dispersion is possible for instruments with diffraction grating upon transition to higher-order spectra. However, there is readjustment of different wavelengths of higher order spectra and the free spectral range decreases. The use of crossed dispersion is also related to complication of the optical system and to an increase of the overall dimensions of the instrument.

The method of increasing the angular dispersion of the optical system, which we selected [6], is based on reflection of the spectrum from a spherical surface. The spectrum of visible light, shaped by a classical optical system, is focused on the focal plane of the camera objective, where a cylindrical mirror (TsZ), the generatrix of the cylindrical surface of which is located in a plane perpendicular to the plane of dispersion of the dispersing element, at an angle to propagation of the beam. Parallel beams with specific dispersion are reflected from the surface of the cylindrical mirror at different angles, due to which the angular distance between beams with wavelength λ and $\lambda + d\lambda$ increases, which also guarantees and increase of the linear dispersion of the system.

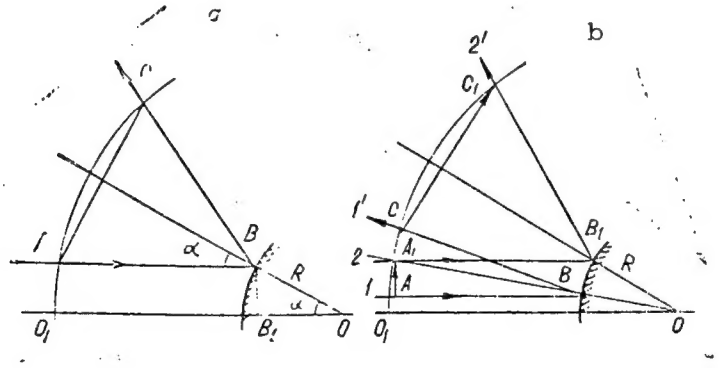

Deflection of Beam From Initial Direction (a) and
Increase of Dispersion of Spectrum (b) Upon Reflection
From Surface of Cylindrical Mirror

One finds from the figure, a, using elementary calculations that deviation of the beam from the initial direction $\Delta H = AC$ upon reflection from the surface of a cylindrical mirror with radius of curvature R at distance L from the cylindrical mirror is expressed by the formula

$$\Delta H = \frac{2LH}{R}, \qquad (2)$$

where $H = BB_1$ is the height of the working surface of the cylindrical mirror from the axis.

The reflection of the region of the spectrum, bounded by beams 1 and 2 from the surface of the cylindrical mirror with radius of curvature R, is shown in figure, b. Taking into account that $L \gg R$, one can assume that $AB = A_1B_1 = L$. Expression (2) for beams 1 and 2 will be in the form

$$AC = \frac{2L}{R} O_1A; \quad A_1C_1 = \frac{2L}{R} O_1A_1$$

The distance between beams 1′ and 2′ dl_2 consists of the total distance between beams 1 and $2dl_1$ and the difference of their deviations (A_1C_1 - - AC)

$$dl_2 = dl_1 + \left(\frac{2L}{R} A_1O_1 - \frac{2L}{R} AO_1\right) = dl_1 + \frac{2L}{R}(A_1O_1 - AO_1)$$

Taking into account that $A_1O_1 - AO_1 = dl_1$, we find

$$dl_2 = dl_1\left(\frac{2L}{R} + 1\right). \qquad (3)$$

Having divided (3) into $d\lambda$, we find the expression of linear dispersion

$$D_2 = D_1\left(\frac{2L}{R} + 1\right). \qquad (4)$$

Hence, it follows that the linear dispersion of an optical system increases $(\frac{2L}{R} + 1)$-fold at distance L after reflection from a cylindrical mirror with radius of curvature R. The validity of expression (4) is easily checked using geometric optics and can be used as a formula for an increase of disperion upon development of spectral instruments by the proposed scheme.

The linear dispersion of an optical system as a dispersing element, on which an Amici prism with base of the main prism of 70 mm was used, could be increased approximately 40-fold and one could find this distance the inverse linear dispersion of 6-8 Å/mm in the entire visible region of the spectrum using a cylindrical mirror 4 mm in diameter at

distance L = 36 mm. Existing instruments with this reverse linear dispersion have considerable overall dimensions and mass [7].

The proposed method of increasing the linear dispersion was caused by an increase of angular dispersion; therefore, it results in a direct increase of the resolution of the optical system. The unilluminated section between the green and yellow lines on the spectrum of a mercury flash lamp is not visually discernible at the output of the above optical system. The distances between these lines are 35 mm after reflection from the surface of a cylindrical mirror with diameter of 5 mm on a screen 5 cm from the cylindrical mirror.

The proposed method can increase the dispersion of any spectral instrument. To do this, one must adapt the cylindrical mirror to the exit slit of the instrument, one must focus the beam with increased dispersion by a lens on a new exit slit and one must calibrate the instrument. The fact that one can increase the dispersion (resolution) of instruments designed to operate in the UV and IR regions of the optical spectrum by selecting a material with good reflectivity to cover the cylindrical mirror also merits attention.

The results of our studies permit one to assume that the proposed method of increasing the dispersion is effective and one can develop small spectral instruments with high resolution on this basis. The economy of these instruments is especially significant in airborne research systems.

BIBLIOGRAPHY

1. Skokov, I. V., "Opticheskiye spektralnyye pribory" [Optical Spectral Instruments], Moscow, 1984.

2. International Application for PCT (WO) No 83/04093.

3. French application No 2,441,155 and No 2,526,942.

4. USSR Inventor's certificate No 1,173,200.

5. GDR patent No 41439.

6. Dilbazov, T. G., "Ustroystvo dlya spektrometricheskikh izmereniy. Polozhitelnoye resheniye na zayavku No 4172443" [Device for Spectrometric Measurements. Positive Solution for Application No 4,172,443].

7. Tarasov, K. I., "Spektralnyye pribory" [Spectral Instruments], Moscow, 1977.

UDC 629.013

Accuracy Characteristics of Optoelectronic Sensor of Roll Control System of Electromagnetically Suspended Model

907F0195A Novocherkassk IZVESTIYA VYSSHIKH UCHEBNYKH ZAVEDENIY: ELEKTROMEKHANIKA In Russian No 7, July 89 (manuscript received 15 Dec 88) pp 64-67

[Article by V. P. Bulekov, and V. S. Volkov]

[Text] A method of arranging the electromagnets in a wind tunnel that permits control of the center of gravity and angular position of the model in the wind tunnel was studied. The control system of the electromagnetic field of the magnets is considered.

Wind tunnels (ADT) with electromagnetic suspension of the air/spacecraft (LA) model are designed to perform aerodynamic tests. Electromagnetic suspension of the LA model in the wind tunnel eliminates the errors introduced by mechanical supports that hold the LA model in it. There are different methods of arranging the electromagnets for suspension of the LA model in the wind tunnel [1]. Most of them use five electromagnets for suspending the model. Four of them are arranged in the upper part of the wind tunnel in two mutually perpendicular planes and are used to suspend the model and to stabilize it along axes y, z according to the angle of attack and yaw angle, while the fifth electromagnet stabilizes the model along axis x and is located in a plane perpendicular to it. This method of arranging the electromagnets does not permit one to control the model by bank angle. Let us consider the following method of arranging the electromagnets to correct this deficiency (Figure 1). Let us install eight electromagnets in four planes and let us arrange them at an angle of 45° to the coordinate planes. Let us connect each pair of electromagnets, mounted in one plane, by a common magnetic circuit, and let us arrange the plane so that they intersect a ferromagnetic core, arranged inside the LA model other than along the axis OX, thus creating a force moment with respect to axis OX when the magnetic flux occurs.

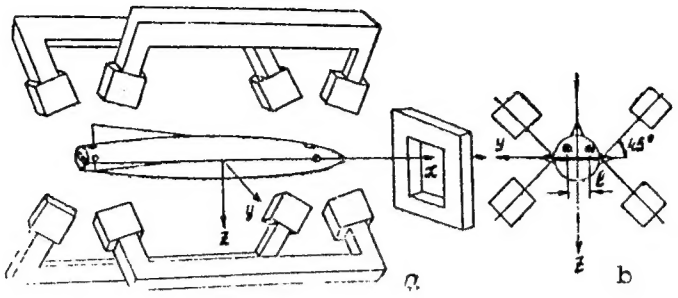

Figure 1. Arrangement of Electromagnets of Wind Tunnel

The control system of the electromagnetic suspension of the model with this method of mounting the electromagnets is a multichannel structure, where each electromagnetic is controlled autonomously as a function of the position of the LA model in space. The electromagnets not only suspend the model in space and control its center of gravity, but can also be used to control it in pitch and bank.

Sensors that measure the linear and angular displacements of the model with respect to the equilibrium position are required to control the position of the model in the wind tunnel. Optical sensors are the most widespread [2]. However, they are not adapted to measure the bank angle. This problem can be solved by using a string optoelectronic sensor (SOED) that permits one to measure the angular displacements of the model and to shift its center of gravity. Let us consider the control system of a model for banking with SOED as the sensitive element that measures the contactless bank angle.

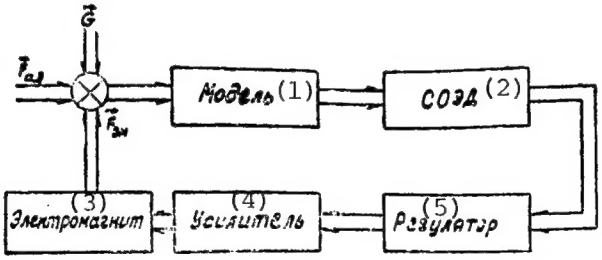

Figure 2. Block Diagram of Control System

KEY:

1. Model
2. String optoelectronic sensor
3. Electromagnet
4. Amplifier
5. Regulator

A block diagram of the control system is presented in Figure 2. It consists of the control object (model), the SOED that measures the bank

angle and that converts it to an electric signal, a regulator that shapes the voltage according to the selected law of control, a power amplifier and electromagnets that create a force acting on the model to eliminate the resulting deviation of the model. The SOED consists of a light source that illuminates marks applied to the model, an objective, a string modulator, photodetector, data processor, and generator (Figure 3). The mark is a light or dark line on a dark or light background. The string modulator is made in the form of a string, stretched between the permanent magnets. A sinusoidal current is passed along the string from a generator, which results in periodic vibrations of the string. Pulse-time modulation is used in the SOED. The bank angle is measured in the following manner: the images of the marks are constructed by the objective in the vibration plane of the corresponding string modulators. The vibrating string periodically covers the image of the mark line, changing the value of the luminous flux at the moment of overlap and, thus creates photopulses. Information about displacement of the image of the mark line with respect to the vibrational axis of the string is embedded in time interval t_1 and t_2 between two adjacent photopulses (Figure 4). Since the string performs harmonic vibrations, the dependence of displacement a_{CM} of the image of the mark line with respect to the vibrational axis of the string on the time interval has the form:

$$a_{cm \cdot n} = A_0 \sin\left[\frac{\pi}{2T_c}(t_2 - t_1)\right], \qquad (1)$$

where n is the number of the mark, displacement of which is determined, A_0 is the vibration amplitude of the string, and T_C is the period of vibration of the string. The data processor converts the signals on displacement of two marks a_{CM1} and a_{CM2} to a bank angle γ by the formula:

$$\gamma = \operatorname{arctg}(a_{cm1} - a_{cm2})/l,$$

where l is the linear distance between marks (Figure 1, b).

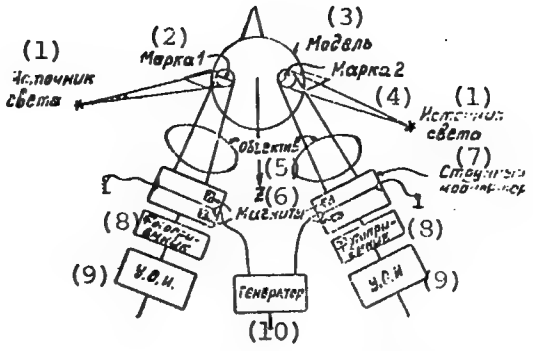

Figure 3. Diagram of String Optoelectronic Sensor

KEY:

1. Light source
2. Mark 1
3. Model
4. Mark 2
5. Objective
6. Magnets
7. String modulator
8. Photodetector
9. Not further identified
10. Generator

The accuracy of the SOED is mainly dependent on the frequency stability of the generator, on the constancy of the vibration amplitude of the string, and on the accuracy of measuring the time interval. Displacement (1) of the image of the mark line will be determined with regard to the error by the formula:

$$a_{\text{см } n} \pm \sigma = (A_0 \pm \Delta) \times \times \sin\left[\frac{\pi(t_2 - t_1 \pm \delta)}{2(T_c \pm \xi)}\right],$$

where σ is the error of measuring the displacement of the image of the mark, Δ is the instability of the vibration amplitude of the string, δ is the error of measuring the time interval ($t_2 - t_1$), and ξ is the instability of the generator frequency. Hence, the error of measuring the displacement of the image of the mark will be:

$$\sigma = 2A_0 \cos\frac{\pi[2(t_2 - t_1) \pm \delta \pm \xi(t_2 - t_1)/T_c]}{4(T_c \pm \xi)} \sin\frac{\pi[\pm\delta \mp \xi(t_2 - t_1)/T_c]}{4(T_c \pm \xi)} \pm \pm \Delta \sin\frac{\pi[(t_2 - t_1) \pm \delta]}{2(T_c \pm \xi)}. \quad (2)$$

Under boundary conditions, when $t_2 - t_1 = 0$, we have:

$$\sigma=(A_0 + \Delta)\sin\left[\frac{\pm\pi\delta}{2(T_c\pm\xi)}\right].$$

When t_1 or t_2 is equal to zero, that is, when $t_2 - t_2 = T_c$, we have

$$\sigma = 2A_0\cos\frac{\pi(2T_c\pm\delta\pm\xi)}{4(T_c\pm\xi)}\times$$

$$\times\sin\frac{\pi(\pm\delta-\xi)}{4(T_c\pm\xi)}+\Delta\sin\frac{\pi(T_c\pm\delta)}{2(T_c\pm\xi)}.$$

The error of modern generators is $\xi = \pm 10^{-4}$ Hz, while modern measuring devices permit one to measure the time interval with an error of $\delta = \pm 10^{-3}$ s [3]. Therefore, one can assume in practice that $\xi = 0$ and $\delta = 0$, and (2) then assumes the form:

$$\sigma = \Delta\sin\pi(t_2 - t_1)/2T_c. \qquad (3)$$

Being given the values of the period of vibration of the string, the values of instability of the vibtration amplitude of the string and assuming, for example, that the minimal measured interval $t_2 - t_1 = 10^{-5}$ s, $T_c = 10^{-3}$ s, and $\Delta = 0.5\cdot10^{-3}$ m, we find from formula (3) the error in measurement of the displacement of the image of the mark in the vibration plane of the string equal to $\sigma = 0.14\cdot10^{-6}$ m, which comprises an error in determination of the displacement of the model (mark) $\sigma = 1.4\cdot10^{-6}$ m at distance of up to 0.5 m to the mark and at focal distance of the objective of 0.05 m, and this is 0.6" in angular measure. The graph of the dependence of the accuracy of determining the displacement of the image of the mark line on the instability of the vibration amplitude of the string at different periods of vibration of the string is presented in Figure 5.

Analysis of the function shows that the accuracy of determining the displacement of the sensor deteriorates sharply as the period of vibration of the string decreases and as the instability of the vibration amplitude of the string increases at the minimum measured time interval $t_2 - t_1 = 10^{-5}$ s. It should also be noted that the instability of the vibration amplitude of the string hardly affects the accuracy of the SOED with a vibration period of the string of $T_c = 2\cdot10^{-3}$ s.

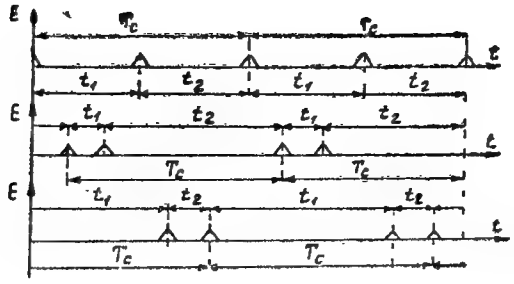

Figure 4. Graph of Shaping of Pulses by String Modulator

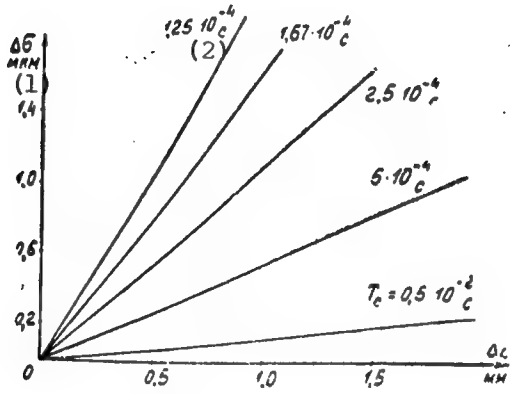

Figure 5. Graph of Dependence of Accuracy in Determination of Displacement of Image of Mark Line on Instability of Vibration Amplitude of String

KEY:

1. μm 2. s

It should be noted in conclusion that the proposed method of arranging the electromagnets in combination with a high-precision SOED in the control system of an electromagnetic suspension permits one to perform aerodynamic tests of LA models over a wide range with stable suspension of the LA model.

BIBLIOGRAPHY

1. Obzor TsAGI, No 557, 1979.

2. Katsnelson, O. G. et al., "Avtomaticheskiye izmeritelnyye pribory s magnitnoy podveskoy" [Automatic Measuring Instruments With Magnetic Suspension], Moscow, Izdatelstvo "Energiya", 1970.

3. "Izmereniya v elektronike. Spravochnik" [Measurements in Electronics, a Handbook], edited by V. A. Kuznetsov, Moscow, Energoatomizdat, 1987.

UDC 621.311.25:621.039

Study of Separation and Hydrodynamic Characteristics of Steam Generator of Serial Unit of AES With VVER-1000

907F0208A Moscow ELEKTRICHESKIYE STANTSII in Russian No 1, Jan 90 pp 29-33

[Article by A. G. Ageyev, doctor of technical sciences, B. M. Korolkov, candidate of technical sciences, V. G. Dants, P. L. Ipatov, engineer et al., ENIN, VNIIAM, Minatomenergo SSSR, Gidropress, and Balakovskaya AES]

[Text] The problem of developing a VVER-1000 section of increased reliability determined the need for further improvement of the design of PGV-1000 steam generators (PG) and of improving their technical and economic indicators. Further optimization of individual design solutions, especially of those which influence the processes and output design characteristics of steam generators, is feasible.

Studies of the PGV-1000 with perforation of swimming-pool plates (PDL) 3.7 and 6.1 percent on the fifth unit of the Novo-Voronezh AES revealed the presence of discharge of a steam-water mixture from the space between the steam generator shell and the flange PDL on the side of the inlet ("hot") coolant header when the electric power unit reaches approximately 80 percent of the rated value, which has a negative influence on the process of gravity separation.

Installation of deflecting baffles in front of the extreme units of the baffle separator on the side of the "hot" header made it possible to protect the baffles from the direct effects of moisture, delivered to the steam space from this gap, thus providing normalized steam moisture content beyond the steam generator at rated power and at the design level of the water [1]. However, installation of a deflecting baffle, having eliminated the consequences of discharge of steam, resulted in the appearance of a transverse steam flow, deflected from the baffle in the steam generator, having distorted the hydrodynamics of the bubbling layer above the PDL and having deteriorated the steam separation conditions. The use of a deflecting baffle also did not eliminate the other negative effect, related to discharge of steam and which included increased steam content (up to approximately 80 percent) in the descending space between the end of the PDL and the heat transfer bundle from the direction of the "hot" header [2]. An increase of the degree

of preparation of the PDL to 7-8 percent did not solve the problem of discharge of steam from under the "hot" edge of the PDL. Moreover, calculated estimates and experiments, performed on a model of the PGV-1000 without leakage of steam under the edge of the PDL and with uniform loading of the evaporation surface, show the possibility of implementing a separation scheme without a baffle separator with overhead perforated panel (PDShch), used successfully on the separator drums of power-generating units of AES with RBMK reactors. Therefore, elimination of steam discharge and equalization of the steam load of the evaporation surface in the PGV-1000 is a necessary condition for considerable simplification of the separation scheme of a steam generator by replacing the baffle separator with an overhead perforated plate. The feasibility of this replacement was also noted in [3].

The simplest technical solution that permits one to prevent the steam-water flow from entering the mentioned space in the steam volume is overlapping the space along the entire generatrix of the steam generator with additional perforated plates. Water would drain from the PDL only along its ends and from the direction of the outlet ("cold") coolant header, which essentially corresponds to the actual pattern of movement of the flows. The proposed measure to eliminate discharge of the steam-water mixture should naturally in no way worsen the hydrodynamic situation in any zone of the water volume of the steam generator, compared to its standard design.

Separation and hydraulic tests of the steam generator, on one of which (PG-4) the space between the steam generator show and the edge of the PDL in the direction of the "hot" header was closed by additional plates with approximately 8 percent perforation, were conducted in the first unit of the Balakovskaya AES. The end sections of this space were covered by solid plates, while windows provided by the design were open in the upper part of the edge to release steam. The PG-4 was supplied with a system of experimental monitoring sensors to check the efficiency of the proposed design solutions (Figure 1). A total of six samplers was mounted above the PDL to determine the separation characteristics of the steam volume. The samples of wet steam were taken from the most typical zones of the steam volume, including that from under the deflecting baffle (No 1), at the elevation below the edge of the baffle in the direction of the "hot" header (No 5), and also along the same vertical 180 and 380 mm below the baffle (Nos 4 and 3), and 380 mm below the baffle in the direction of the "cold" header (No 6).

A total of 10 hydrostatic steam content sensors and 5 turbine flowmeters were located in different zones of the water volume of the steam generator to measure the circulation parameters.

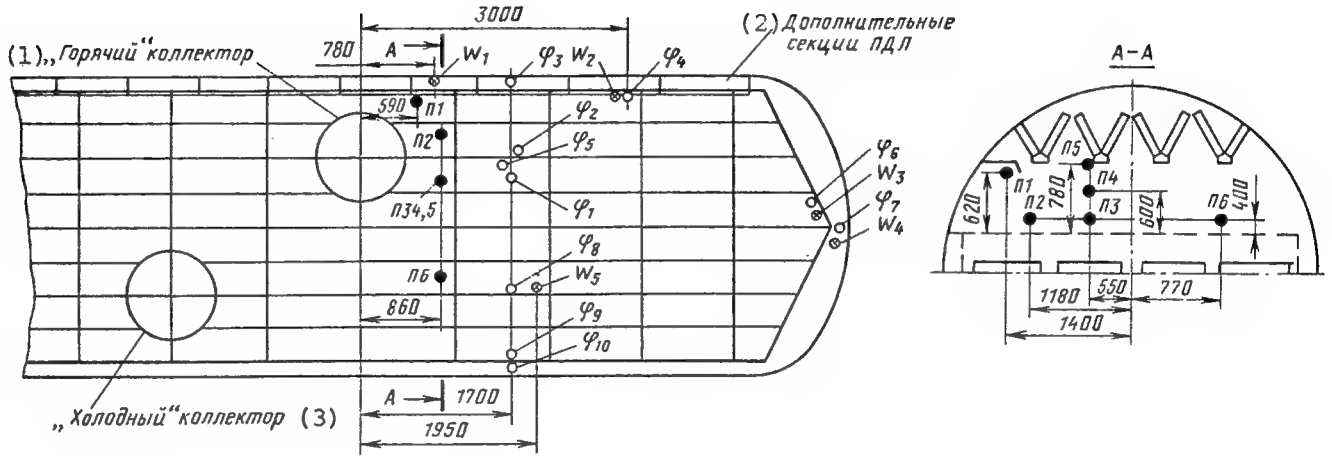

Figure 1. Layout of Experimental Monitoring Sensors in Shell of PG-4:
●--sampler; O--steam content sensor; ⊠--flow rate sensor

KEY:

1. "Hot" header
2. Additional sections of PDL
3. "Cold" header

Separation and thermal tests of all the remaining steam generators of the unit were performed in parallel with the study of the separation and hydrodynamic characteristics of the PG-4 for comparative analysis using standard measuring devices. The tested steam generators had average perforation of the PDL of approximately 7.3 percent.

The saline method was used to measure the moisture content. Sodium nitrate, a solution of which was introduced into the steam generator to be tested together with feedwater in an amount that guarantees sodium concentration of 20-25 mg/liter in the water volume of the steam generator during the measurements, was used as the salt indicator. The sodium concentration in the samples was determined on a PAZh-2 flame photometer.

Hydrostatic sensors, made in the form of a pair of static pressure samples with base of 200 mm (sensors Nos 1 and 2) and 700 mm (sensors Nos 3-10) were used to measure the true volumetric steam content $\bar{\varphi}$. The top pressure bleeds of sensors with a base of 700 mm were located approximately 100 mm from the elevation level of the PDL. The installed sensors permitted one to measure $\bar{\varphi}$ in all the typical zones of the water volume of the steam generator: under the PDL, in the "hot" and "cold" corridors, in the region of the "hot" edge and in the "hot" end of the steam generator. Sapfir pressure drop meters in a set with KSU potentiometers were used as the secondary apparatus.

Turbine flowmeters were installed along both sides of the "hot" edge and in the "hot" end of the steam generator to measure the flow rate and direction of flow in the "cold" discharge corridor of the tube bundle. The signals of the sensors were recorded on a loop oscillograph of type N.071.1. The design ofthe flowmeter, its service life and set of secondary apparatus were certified under bench conditions at the rated operating parameters of the steam generator. Sensors 1, 3 and 5 were located 650 mm, while sensors Nos 2 and 4 were located 350 mm from the level of the PDL plate.

The separation and thermohydraulic characteristics of the steam generator were studied over a wide range of variation of electric power, beginning with MKU modes up to output of the unit to rated electric power. The main volume of data was obtained at the electric power level of the unit of 90 and 100 percent of the rated value. The thermal operating efficiency of the steam generators, their actual steam productivity and a check of the thermal power through the circulating loops were first estimated.

The values of the heat transfer coefficients, obtained from the test data, correspond to the calculated values for an unloaded heating surface (approximately 6,000 $W/m^2 \cdot K$), which corresponds for the period of developing the designed power to the results of earlier studies of the PGV-1000 [1], while a check of the thermal power through the circulating loops comprises an average of 7-8 percent. The steam

productivity of the PG-3 and PG-4 was 106 and 104 percent, respectively, of the rated value and the steam productivity of the PG-1 and PG-2 was somewhat below the rated value at rated electric power of the unit.

The separation characteristics of the PG-4 and PG-3 steam generators, having approximately identical steam load, are presented in Figure 2 and the form of the dependence of the steam moisture content in the steam line beyond the steam generator on the water level, measured by a standard level meter on the BShchU (position L 19, "cold" end), at electric power of the unit of 90 and 100 percent of the rated value. The minimum steam moisture content occurs in both cases for a PG-4, supplied with additional PDL plates. For this steam generator, the steam moisture content at maximum water level of 2.6 m and at electric power of the unit of 100 percent is equal to approximately 0.4 percent, whereas it comprises approximately 1 percent for the PG-3. The separation characteristics of the PG-1 and PG-2, despite the rather narrower steam load, was also worse than that for the PG-4, supplied with additional PDL plates.

The results of measuring the moisture content in the steam volume of the PG-4 are presented in Figure 3 as a function of the position of the level on the level meter of the BShchU at electric power of the unit of 90-92 and 95-100 percent. It follows from consideration of the data that the separation characteristics of the steam volume at different height elevations and the positions of water level on these characteristics have a form typical for operation of the gravity volume. This indicates the absence of an interruption of steam from under the "hot" edge of the PDL, which previously resulted in abnormal distribution of moisture content along the height of the steam volume and about equalization of the load of the evaporation surface.

A monotonic increase of moisture content through all samplers is observed with an increase of water level and a sharp increase of moisture content begins earlier, the lower the sampler is located with respect to the PDL. The fact that moisture content through sampler No 1 under the baffle is less than that through sampler No 4, located at approximately the same elevation marker, but closer to the longitudinal axis of the steam generator, is noteworthy. This directly indicates total elimination of the discharge of steam-water flow from the "descending" space on the "hot" side of the steam generator, and also the fact that the load of the evaporation surface on the periphery of the steam generator in the zone of installation of sampler No 1 is less than that in the region of sampler No 5.

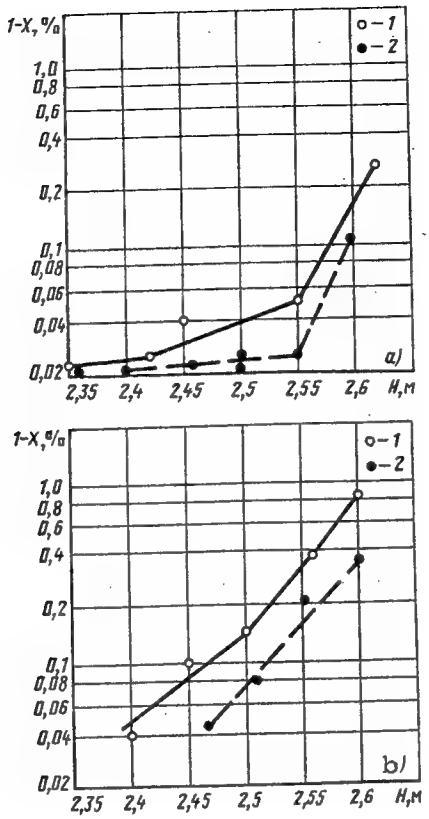

Figure 2. Graphs of Dependence of Steam Moisture Content in Steam Line Beyond Steam Generator on Water Level: a--at 90 percent electric power of unit: 1--PG-3, $G/G_{НОМ}$ = 98 percent; 2--PG-4, $G/G_{НОМ}$ = 97 percent; b--at rated electric power of unit: 1--PG-3, $G/G_{НОМ}$ = 106 percent; 2--PG-4, $G/G_{НОМ}$ = 104 percent

The dependence of the moisture content in the steam volume of the PG-4 from samplers Nos 1, 4 and 5, compared to data obtained in similar zones on one of the steam generators (PG-3) of the fifth unit of the Novo-Voronezh AES, are presented in Figure 4. It follows from comparison of the graphs that the level of the moisture content at the elevation of the lower edge of the baffle (sampler No 5) decreased considerably after installing additional PDL plates, which naturally explains the lower level of moisture content in the steam line of PG-4 compared to the other steam generators. The moisture content in PG-4 also decreased in samplers Nos 1 and 4, the high value of which in the PG-3 of the Novo-Voronezh AES is also explained by the presence of a steam-water flow, reflected by the baffle, in the steam volume of the steam generator.

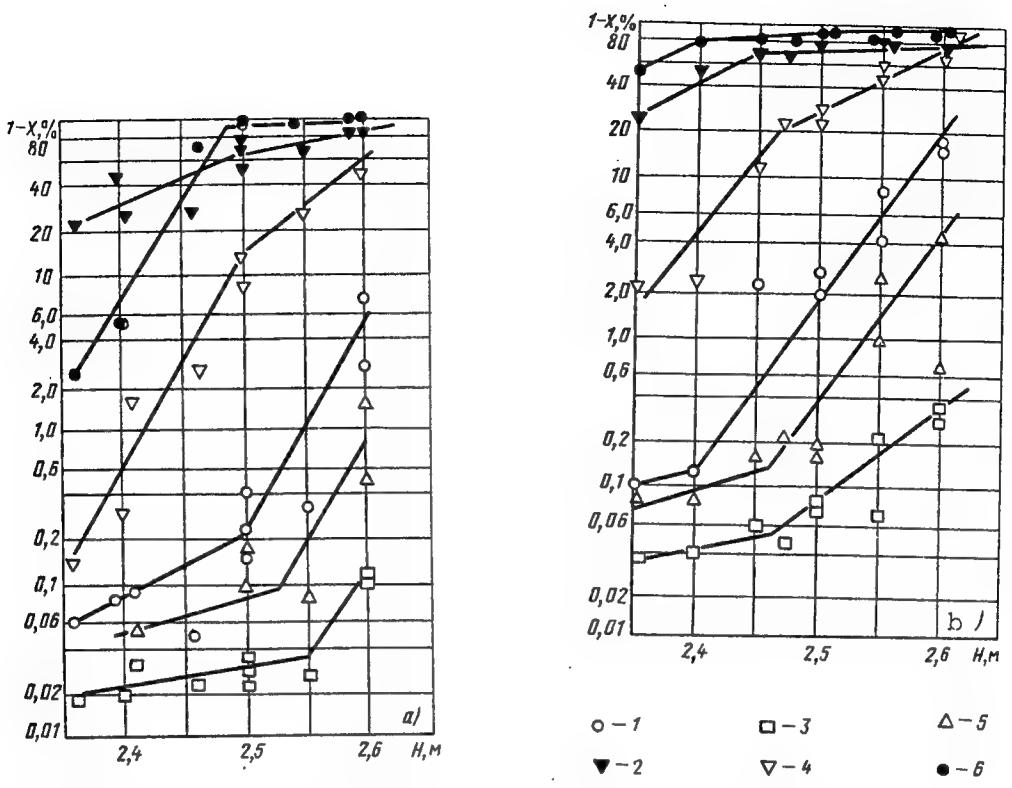

Figure 3. Graphs of Dependence of Steam Moisture Content in Different Zones of Steam Volume in Steam Line of PG-4 on Water Level:
a--at electric power of unit of 90-92 percent; b--at electric power of unit of 95-100 percent; 1--sampler No 1; 2--sampler No 2; 3--in steam line; 4--sampler No 4; 5--sampler No 5; 6--sampler No 6

The data found in this study on the values of the true volumetric steam content and rates of circulation in the water volume of the steam generator and on the influence of the power and water level as a whole on these characteristics are in qualitative agreement with the experimental data [2]. Data of this study and those found in [2] for identical zones of the steam generator are presented in the table to determine the possible quantitative differences.

(1) Зона расположения датчика	(3)	(2) Истинное объемное паросодержание φ		(5) Скорость потока w, м/с	
		(3) Балаковская АЭС (ψ=7,3 %)	(4) Ново-Воронежская АЭС [2] (ψ=3,7 %)	(3) Балаковская АЭС (ψ=7,3 %)	(4) Ново-Воронежская АЭС [2] (ψ=3,7 %)
Над трубным пучком	(6)	0,6	1,0	—	—
Над «горячим» коридором	(7)	0,48	—	—	—
Корпус — закраина («горячая» сторона)	(8)	0,65	0,75—0,8	$w\uparrow$=0,85; $k\uparrow$=0,75 $w\downarrow$=0,35; $k\downarrow$=0,03	$\bar{w}\uparrow$=1,0
Пучок — закраина («горячая» сторона)	(9)	0,53	0,8 ($\bar{\psi}$=6,1 %)	$w\uparrow$=1,6; $k\uparrow$=0,8; $w\downarrow$=0,8; $k\downarrow$=0,05;	—
«Горячий» коридор	(10)	0,56	0,55	—	$\bar{w}\downarrow$=0,3
Пучок — закраина («горячий» торец)	(11)	0,37	—	$w\downarrow$=0,8; $k\downarrow$=0,8 $w\uparrow$=0; $k\uparrow$=0;	—
Корпус — закраина («горячий» торец)	(12)	0,35	—	$w\downarrow$=0,47; $k\downarrow$=0,2; $w\uparrow$=0,53; $k\uparrow$=0,36	—
Корпус — закраина («холодный» торец)	(13)	—	0,15—0,2	—	$\bar{w}\downarrow$=0,25 $\bar{w}\uparrow$=0,02
«Холодный» коридор	(14)	0,45	0,53	$w\uparrow$=0,30; $k\uparrow$=0,1 $w\downarrow$=0,4; $k\downarrow$=0,4	$\bar{w}\downarrow$=0,6
Пучок — закраина («холодная» сторона)	(15)	0,45	—	—	—
Корпус — закраина («холодная» сторона)	(16)	0,40	0,37	—	—

KEY:

1. Location of sensor
2. True volumetric steam content
3. Balakovskaya AES
4. Novo-Voronezh AES
5. Flow rate w, m/s
6. Above tube bundle
7. Above "hot" passageway
8. Shell-edge ("hot" side
9. Bundle-edge ("hot" side)
10. "Hot" passage
11. Bundle-edge ("hot" end)
12. Shell-edge ("hot" end)
13. Shell-edge ("cold" end)
14. "Cold" passage
15. Bundle-edge ("cold" side)
16. Shell-edge ("cold" side)

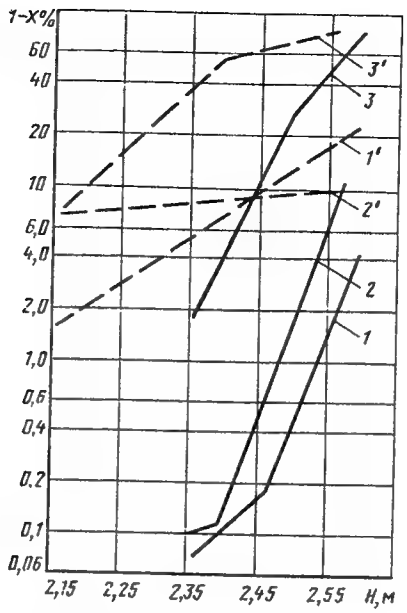

Figure 4. Graphical Comparison of Steam Moisture Content in Identical Zones of Water Volume of Steam Generators of Balakovskaya and Novo-Voronezh AES at Rated Electric Power of Units:
1--moisture content on lower edge of baffle (PG-4, first unit of Balakovskaya AES, sampler No 5); 1'--the same for PG-3, fifth unit of Novo-Voronezh AES; 2--moisture content under baffle (PG-4, first unit of Balakovskaya AES, sampler No 1); 2'--the same for PG-3, fifth unit of Novo-Voronezh AES); 3--moisture content in volume of steam generator at height of 0.6 m from PDL (PG-4, first unit of Balakovskaya AES, sampler No 4); 3'--the same for PG-3, fifth unit of Novo-Voronezh AES

Comparison of the data with respect to $\bar{\varphi}$ shows that installation of additional PDL plates essentially had no effect on the steam content in the intertube "descending" corridors from the "hot" and "cold" directions and in the space between the edge of the PDL and the shell of the steam generator from the "cold" direction. Some quantitative differences of $\bar{\varphi}$ for the steam generators of the Balakovskaya and Novo-Voronezh AES occur for two zones of the steam generator:

in the region of the edge on the "hot" side of the steam generator, above the tube bundle 1,700 mm from the axis of the "hot" header (sensor No 1 of the Balakovskaya AES, see Figure 1) and 1,220 mm (sensor of the Novo-Voronezh AES).

Specifically, the steam content in the space between the "hot" edge of the PDL and the heat-transfer bundle decreased from 0.8 to 0.53 after installation of additional PDL plates. This fact is unconditionally positive, since it guarantees more favorable operating conditions of the heat-exchange bundle in this part of the steam generator. The steam content between the shell and "hot" edge also decreased somewhat. It follows from comparison of the experimental values of $\bar{\varphi}$ above the tube bundle that the steam content sensors of the Novo-Voronezh AES record formation of a stable "steam cushion" ($\bar{\varphi}$ = 1.0) in this zone of the steam generator (at $\bar{\varphi}$ = 3.7), whereas the value of $\bar{\varphi}$ comprises 0.6 from the readings of the sensor of the Balakovskaya AES. The indicated quantitative difference is apparently related both to installation of additional PDL plates on the steam generator of the Balakovskaya AES and to the different degree of perforation of the PDL in both studies. As a whole, the data of this study with respect to $\bar{\varphi}$ above the heat exchange bundle indicate the absence of prerequisites of "steaming" of its top rows.

The values of coefficients $k\uparrow$ and $k\downarrow$, which characterize the temporary contribution of the given direction of flow to the total length of the recorded signal, are presented in the table upon representation of the experimental data of this study with respect to the flow rates under conditions of different movement of the medium, besides the absolute values of the rate of the ascending $w\uparrow$ and descending $w\downarrow$ flows. Transition to the mean flow values $w\uparrow$ and $w\downarrow$, which permit one to judge to a known degree the intensity of the circulation in the corresponding zones of the steam generator, can be achieved by simple relations

$$\bar{w}\uparrow = w\uparrow k\uparrow;$$
$$\bar{w}\downarrow = w\downarrow k\downarrow.$$

Direct comparison of the flow rate to data of [2] can be performed for two zones of the steam generator: between the shell and the edge in the direction of the "hot" header and in the "cold" passage.

Ascending motion of the flow at approximately identical rates is recorded in the first of the zones in both studies. The second zone is characterized by primarily descending movement of the flow in the zone of installation of sensor w_5 in PG-4 of the Balakovskaya AES (see Figure 1) and by stable nonfluctuating descending motion of the medium at the point of installation of the flow rate sensor of the Novo-Voronezh AES (the sensor is located near the "cold" header).

The very high values of the flow rate, recorded in this study by the sensor located in the space between the bundle and edge in the direction of the "hot" header, are explained by the location of the sensor directly in the region of the open window of the edge and which

therefore experiences the effect of the steam flow from the shell-edge region. Movement of the medium in different directions and recorded by the sensors located between the shell and the edge in the end zones of the steam generator is determined by drainage of the water flow from the PDL and by periodic floating of steam bubbles, captured in this space. As a whole, the considered data on the flow rate indicate that no significant differences are observed in the nature of circulation of the flow in the water space of the PG-4 of the first unit of the Balakovskaya AES, supplied with additional perforated plates, compared to steam generators of the fifth unit of the Novo-Voronezh AES.

Returning to the graphs of Figure 3 on the separation characteristics of the PG-4, one can conclude that the moisture content in the steam line essentially "follows" its value on the bottom edge of the baffle (sampler No 5, see Figure 1). The low moisture content in the steam line is also recorded with a low value of moisture content in this zone of the steam generator. The moisture content in the steam line essentially increases simultaneously as the moisture content on the bottom edge of the baffle increases with the increase of level. This ratio of the dependence of moisture content on the level before and after the baffle separator is typical when it is used in combination with the free steam volume. Therefore, the baffle, having a natural height of 500 mm in the PGV-1000 steam generator can fail, since the height of the steam volume will increase accordingly, and the separation conditions will be improved and the maximum position of the mass water level above the PDL will increase, as calculations and bench experiments show.

Conclusions

1. Installation of additional PDL plates above the space between the steam generator shell and the edge of the PDL from the direction of the "hot" coolant header made it possible to completely eliminate the discharge of the steam-water mixture from this space, which resulted in a considerable decrease of moisture content at the inlet to the baffle separator, to improvement of the steam separation conditions and to a guarantee to a lower level of moisture content in the steam line, compared to PGV-1000 steam generators of standard design.

2. Installation of additional PDL plates caused no changes of the hydrodynamics of the water volume of the steam generator, compared to its standard version. At the same time, the steam content in the space from the "hot" direction between the direction of the PDL and the heat-exchange bundle decreased from 0.8 to 0.5 and this is favorable for circulation conditions in this part of the steam generator.

3. Elimination of the discharge of the steam-water mixture to the steam volume opens the possibility of conducting an industrial experiment on the existing steam generator to replace the baffle separator by an overhead perforated panel. This replacement permits one to improve the technical and economic indicators of the PGV-1000 steam generator and to

expand the permissible range of variation of the level by essentially doubling the proposed height of the steam volume and to increase considerably the margin in the productivity of the steam generator.

BIBLIOGRAPHY

1. Tarankov, G. A., V. F. Titov, S. A. Logvinov et al., "Study of Steam Generator of Pilot Unit of AES With VVER-1000," ENERGOMASHINOSTROYENIYE, No 5, 1986.

2. Ageyev, A. G., R. V. Vasilyeva, A. I. Dmitriyev et al., "Study of Hydrodynamics of PGV-1000 Steam Generator," ELEKTRICHESKIYE STANTSII, No 6, 1987.

3. Margulova, T. Kh. and V. F. Titov, "On Improving the Separation Characteristics of the Steam Generators of AES With VVER Reactors," TEPLOENERGETIKA, No 11, 1984.

UDC 621.311.22:658.5.011.56

Realization of Algorithm for Recording Emergency Situations in Process Control Systems of 300-MW Power-Generating Unit

907F0208B Moscow ELEKTRICHESKIYE STANTSII in Russian No 1, Jan 90 pp 73-75

[Article by V. Kh. Sopyanik, candidate of technical sciences, A. M. Mazurov, engineer, and G. T. Mindiyarov, engineer, Western Branch of All-Union Heat Engineering Institute imeni F. E. Dzerzhinskiy]

[Text] One of the primary and main information problems which the operational personnel of TES wish to have upon development and introduction of an information computer complex (IVK) of the process control system in power-generating units of TES is recording emergency situations (RAS). This is explained by the fact that existing methods of recording emergency situations using various event recorders, automatic recording instruments and online records in logs are hardly effective, since there is no clear time tie-in, considerable time expenditures are required for processing information with regard to its dispersion on diagram tapes, photographic paper and in the operational log.

The main functions of the task of the RAS are [1, 2]:

accumulation of information in the pre-emergency mode during time $T_д$ and emergency mode during time $T_а$ on the main process (analog) parameters of the power-generating unit and of its main equipment, on the response of the protection and automatic devices, on variation of the state of the switching and shutoff equipment, and of the state of the control keys;

processing the accumulated information and presentation of it to the personnel of the TES in the form of a technical document that provides in convenient form a description of the process of the occurrence, development and elimination of the emergency situation on a given time interval with clear time tie-in of events.

The algorithm for the task of the RAS [1, 2] was realized by the authors on a SM-2M computer with subsystem for communicating with the object

based on the subsystem for communicating with object K332-2 (SSO), in which the information about the passive discrete sensors is introduced by using digital signal switches (KDS) (power-generating units Nos 3, 4, 5, and 6 of the Azerbaijan GRES) and on the SM-2M computer with subsystem for communicating with the object based on RSO (power-generating unit No 1 of the Yuzhnaya TETs of Lenenergo) on the basis of the hardware of the control computer complex of the process control system of power-generating units.

Analog and passive digital data acquisition and processing programs function in the considered control computer complex of the process control system, which gathers data every 5 seconds from the analog sensors (temperature, pressure, flow rate, power, current, voltage and so on) and information about the condition of passive digital sensors (position of slides, cover plates, some switches of low-crucial mechanisms for internal needs and so on), entered in the control computer complex.

Information is entered from the relay and process protection (RZ, TZ) devices, automatic devices (A), and switch-shutoff equipment (switches, shutoff valves and so on) (KZA) into the control computer complex through modules for entry of initiative signals (MVvIS) [2, 3].

The necessary information about the given analog and passive digital sensors for the task of the RAS is selected from files, current values of the analog and passive digital data, shaped by the acquisition programs, by using the sampling programs and is stored in the files of the pre-emergency values of the analog and digital passive data. These files are updated continuously and contain information during the pre-emergency mode $T_{Д}$ = 5-15 min, regardless of when the accident occurs.

When an accident occurs--influx of one or several signals to the information computer complex from the initiative signal input module, to which the output relays of the process protection, relay protection and automatic and switch-shutoff apparatus are connected, which indicate the occurrence of an accident, updating the files of pre-accident information is stopped. The data is rewritten to the floppy disk (NMD) and accumulation of information in the emergency mode is begun by the same scheme during time T_{a} = 10-15 min.

The cyclicity of rewrite of the pre-emergency and emergency information to floppy disk is dependent on the capacity of the main memory, allocated for the RAS task.

The algorithm for the RAS task is realized by a combination of program modules. The program modules, which implement the functions of starting the programs for selection of analog and passive digital data, initiative digital data acquisition and processing, output of online

messages to personnel of the power-generating unit, are permanently in the computer RAM.

The program modules whose function consists in formulation of a document on the accident, are called to the RAM from the floppy disk by the operator of the power-generating unit. Thus, the program modules of the task of the RAS are conditionally divided into RAM-resident and disk-resident, a block diagram of which is presented in Figures 1 and 2. They communicate with each other through a data reference file (ISF).

The following program modules are included in the RAM-resident part: controller of the RAS task (PYSK program), initiative processing program (SBORD), program for selection of analog and passive digital data (VIBOR), and program for output of online messages (VDM).

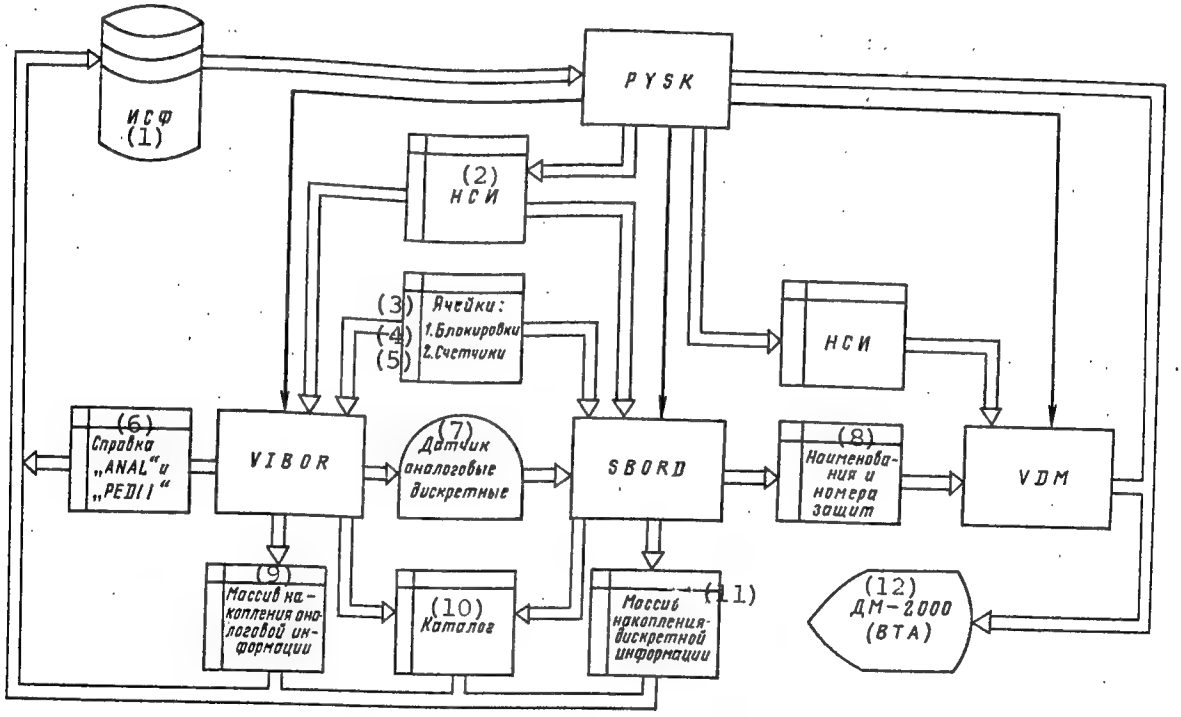

Figure 1. Block Diagram of Algorithm for Functioning of RAS Task (RAM-Resident Part)

KEY:

1. Data reference file
2. Not further identified
3. Cells
4. Lockouts
5. Counters
6. Reference "ANAL" and "PEDII"
7. Analog-digital sensors
8. Names and numbers of protection
9. Analog data storage file
10. Catalog
11. Digital data storage file
12. DM-2000 (VTA)

The functions of the controller of the RAS task includes execution of operations on loading the reference data, preparation of files and of counter cells, of lockout indicators for stopping the functioning of the program components in case of their incorrect functioning or stopping the execution of operations and starting the VDM module to issue messages to the video terminal screen. The set of functions performed by the RAS task controller is dependent on the directive entered by the operator of the power-generating unit in interaction with the PYSK program. Entry of one or another directive is dependent on the specific situation, established at the power-generating unit or during operation of the task (for example, initial start of the RAS task, restart of the task due to soft failures of the computer, floppy disk and so on).

Acquisition of initiative digital data, storage of it, determination of the feature that indicates the occurrence of an accident (response of the TZ, RZ and so on) is entrusted to the programmed initiative processing module SBORD .

The programmed data selection module (VIBOR) selects and stores analog and passive digital data in the RAM files, rewrites them to the ISF as data are filled to the floppy disk, and calculates the time of pre-emergency and emergency periods of the accident on the basis of 5-second cyclicity of its operation.

The VDM program module formulates the table of online messages on the display (DM-2000, VTA and so on), where the main aspects of the emergency situation are reflected (time of occurrence of the accident, name and time of response of the first five protections, end of recording, and also messages on the inefficiency of the data input devices, NMD and so on).

The RAS task envisions recording of five accidents in a row. When information on five accidents has been accumulated, the task is automatically interlocked to output of the message "Catalog overflow" until the output document for at least one of the recorded accidents is issued.

The loaded module of the disk-resisent section of the RAS task is called to find the document on the accident. It consists of the main print segment start program (PECH) and the following disk-resident segments: the segment for interaction with the operator of the power-generating unit (DIAL), the segment for formation and printout of title lists and description of the output documents of the RAS task (TITYL), the segment for formulation and printout of notification of change of state of the TZ, RZ and A, KZA in pre-accident modes (PEDII), and the segment of formulation and printout of information of variation of the main analog parameters of the power-generating unit (ANAL).

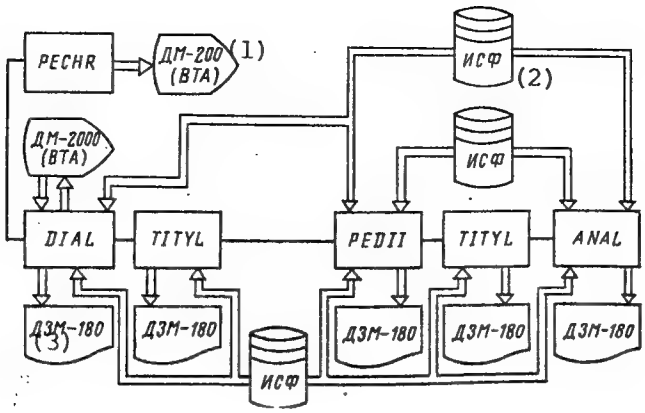

Figure 2. Block Diagram of Algorithm for Functioning of RAS Task (Disk-Resident Part)

KEY:

1. DM-2000 (VTA)
2. Data reference file
3. DZM-180

Specifications of RAS task, realized on basis of subcomplex for communicating with object (SSO) and SM-2M computer in process control system of 300-MW power-generating unit. The RAS task envisions monitoring and recording of the variation of 640 digital sensors (512 passive and 128 initiative) and stores the values of 120 analog parameters. Similar specifications of the RAS task, realized on the basis of the terminal for computer communications with the object (TVSO) and the SM-2M computer, comprise 1,424 digital sensors (1,024 passive and 400 initiative) and 250 analog parameters. The accuracy of tying the variation of state of the digital sensors, entered on the MVvIS, to real time comprises 8 ms. The frequency of interrogation of the analog and passive digital sensors is equal to 5 s. The time during which the RAS task accumulates data in pre-accident and accident modes is equal to $T_д + T_а = 10 + 10 = 20$ min.

It should be noted that the rate of variation of currents, voltages, and power in the emergency modes of the electric part of this plant determines the need for accelerated recording of them compared to interrogation of the given parameters, taken for realization of PCS functions in the part of the information computer complex. Accelerated interrogation should encompass a comparatively small number of analog parameters (10-20 units) with frequency on the order of 0.001 s over a time of $T_{ay} = 0.5$-1 s.

The parameters subject to accelerated interrogation in the emergency mode are connected to one input subsystem with one-step switching. The command system of the TVSO is expanded by special commands for

communicating with the object, which guarantees input of data from one analog sensor within 30 μs from the moment the interrogation appears at the data input until it is entered in the accelerated interrogation task buffer.

The program for accelerated interrogation of analog parameters is started from the start device--the MVvIS, to which are connected digital sensors that indicate the occurrence of an accident or abnormal mode in the electric part of the power-generating unit, for example, the oscillograph start device in the generator monitoring system, and the RZ and A start members or the signals of other digital sensors).

The requested information is stored in codes in the RAM in the accelerated interrogation files of analog parameters during time T_{ay}.

The interrogation is completed within a given time and the data is rewritten from the RAM to the emergency analog data file of accelerated interrogation to the NMD.

The stored data are processed and is arranged if need be into a harmonic series and into symmetrical components.

The instantaneous values of currents and voltages are used to construct the corresponding oscillograms of transient processes.

Information of accelerated interrogation of electric analog parameters is designed to analyze the behavior of the RZ and A devices, for diagnosis of the generator, transformer, switches, and to analyze the emergency processes in the power system.

Unfortunately, the absence of industrially manufactured sensors of the instantaneous values of currents, voltages, and power does not at present permit one to realize the accelerated interrogation algorithm in emergency situations of electric analog parameters in the information computer complex of the process control system, as the typical RAS algorithm recommends [1].

The RAS task formulates the following output data on the accident:

1. The information of state of all the digital sensors for the beginning of the pre-accident mode.

2. Inforamtion of the variation of states of the digital sensors in the pre-accident and accident modes during $T_{Д} + T_{а} = 20$ min.

3. Information of the values of the analog parameters in the pre-accident and accident modes on the boiler unit, turbounit, and generator.

The realized algorithm of the RAS task based on the TVSO and SM-2M computer, should be used in modification of the monitoring and control systems of 300-MW power-generating units based on TVSO.

BIBLIOGRAPHY

1. "Tipovoy algoritm registratsii avariynykh situatsiy energoblokov 300-1,200 MVt TES" [A Standard Algorithm for Recording Emergency Situations of 300- to 1,200-MW Power-Generating Units of Thermal Power Stations], Book 1, Moscow, Proceedings of Teploelektroproyekt, 1980.

2. Senyagin, Yu. V., V. Kh. Sopyanik, Yu. A. Oreshkin et al., "On Recording Emergency Situations in the Process Control Systems of Thermal Power Plants," ELEKTRICHESKIYE STANTSII, No 11, 1982.

3. Yermakov, V. S., V. V. Pazukhin, Yu. V. Senyagin et al., "Avtomatizatsiya upravleniya tekhnologicheskimi protsessami na elektrostantsiyakh s primeneniem sredstv vychislitelnoy tekniki" [Automation of Process Control at Electric Power Plants Using Computer Technology], Moscow, Informenergo, 1986.

UDC 658.012.2

Construction of Optimal Operating Schedule of Flexible Automated Section

907F0190A Minsk IZVESTIYA AKADEMII NAUK BELORUSSKOY SSR: SERIYA FIZIKO-TEKHNICHESKIKH NAUK in Russian No 4, Oct-Dec 89 (manuscript received 5 May 88) pp 104-109

[Article by M. Ya. Kovalev, O. A. Kuznetsova, O. M. Podolinnyy, and Yu. N. Sotskov, Institute of Engineering Cybernetics, BSSR Academy of Sciences, and Scientific Production Association Orbita]

[Text] An organizational-economic management system of a flexible automated section (GAU) for machining is considered. Main attention is devoted to problems of operational-calendar planning (OKP). The problem of compiling a schedule that minimizes the total penalties for violation of directive deadlines of fulfilling the jobs and their total length is postulated. The algorithms and programs for solving this problem and also the experience of practical operation of them are discussed.

1. Problems of OKP. Organizational economic management includes the following main phases of the OKP: monthly production planning, compilation of optimal equipment operating schedule and daily shift planning. The nomenclature plan of the enterprise is made more specific in the first of them according to the operations and dates of their start-output. Optimal distribution of machine tool operations and calculation of the time of the beginning and end of completing them are achieved in the second phase (an optimal schedule of completing the planned operations is compiled). Operations for inclusion in the shift jobs with regard to the condition of the equipment and supply with resources are selected during daily shift planning on the basis of the compiled schedule.

The second phase of the OKP is more complicated from the algorithmic point of view and is important for improving the productivity of the GAU [1]. The resulting mathematical problems are studied within scheduling theory [2]. As studies showed [2, 3], the complexity of solving these problems is fundamental. This must be taken into account in postulation of the problem of compiling the schedules and when selecting the algorithms of solving them.

2. Problem of compilation of optimal schedule. Let us consider a rather typical class of machining GAU. Let us assume that the section consists of M identical machine tools, 1, 2, ..., L, ..., M. Machine tool L is ready to operate at a given moment of time $T_L \geq 0$. A set of operations N = {1, 2, ..., i, ..., n}, which should be performed on the machine tools of the GAU within a considered planning interval (24 hours, week, month and so on), is determined in the operational plan. Each operation is a continuous process of machining some part h, which can be performed on any of the machine tools. Let X = {1, 2, ..., h, ..., k} be a set of all the given parts. If several operations must be performed on the same part h, the sequence $(i^h_1, i^h_2, \ldots, i^h_{n(h)})$ of performing them is indicated. Subsequently, without limiting generality, let us assume that the operations are numbered in the following manner: $i^1_1 = 1$, $i^h_{j+1} = i^h_j + 1$, $h = \overline{1, k}$, $j = \overline{1, n(h)-1}$, $i^{l+1}_1 = i^l_{n(l)} + 1$, $l = \overline{1, k-1}$.

The time $t_i > 0$ of performing the operation is given for each operation $i \in N$. The time $t_{i\ i+1} \geq 0$, which should pass after completion of i before beginning of i + 1, is known for each pair of sequential operations i and i + 1 on one part. It is assumed that each machine tool can perform no more than one operation simultaneously and the time $\tau_{ij} \geq 0$ of readjusting the machine tool after performing operation $i \in N$ before the beginning of operation $j \in N$ is known.

The moment $d_h \geq 0$ of readiness of part h for machining and the directive deadline $D_h \geq 0$ by which the machining of part h on a given section must be completed are given to guarantee the possibility of matching the production plans of different shops and sections of a given enterprise and also of related enterprises for each part $h \in X$. the value of d_h is the moment of readiness to perform operation $i^h_1 \in N$, while the value of D_h is the moment of time, no later than which the operation $i^h_{n(h)} \in N$ should be completed.

A schedule s* of performing a set of operations N (the machine tool on which the operation should be performed is indicated for each operation $i \in N$ and the moment $t^0_i(s^*)$ of the beginning of performing it is indicated) must be compile, at which all of the above conditions are satisfied and the given specific function F(s) assumes the least value F(s*) on a set of all permissible schedules s.

Both the complexity of the task of compiling the optimal schedule s* and the indicators of the functional quality of the GAU upon realization of schedule s* are dependent on selection of a specific function. It is suggested that the following specific function be used:

$$F(s) = b \sum_{h \in X} z_h(s) + \max_{h \in X} \bar{t}_h(s),$$

where $\bar{t}_h(s)$ is the moment of completion of operation $i^h_{n(h)}$ at schedule s and $z_h(s)$ is the given function of the penalty for disruption of the directive deadline of machining the part $h \in X$:

$$z_h(s) = \begin{cases} \alpha_h(\bar{t}_h(s) - D_h), & \text{if } \bar{t}_h(s) > D_h, \\ 0, & \text{if } \bar{t}_h(s) \leqslant D_h. \end{cases}$$

Here $\alpha_h \geq 0$ is the priority of the part $h \in X$, which is assigned with regard to its importance for the entire manufacturing process and for the relationships between shops and sections and so on. It will be shown below how stability of scheduling can be provided by selection of priorities α_h [4] upon correction of the schedule. Coefficient $b \geq 0$ determines the priority of the total length of the schedule with respect to disruptions of the directive deadlines of machining the parts.

3. Complexity of problem. The GAU described in section 2, from the viewpoint of scheduling theory, can be regarded as a one-stage service system with parallel identical devices (machine tools) and with a set of requirements (parts), on which the ratio of precedence to the organizational schedule of reduction G = (N, U) is given in the form of an aggregate of circuits and of isolated vertices [2]. Here U is a set of arcs of organizational graph G. The formulated problem of constructing an optimal schedule is NP-difficult in the strong sense [2, 3]. The low probability of the existence of an effective (polynomial) algorithm for solving it, i.e., of an algorithm whose cumbersomeness is limited by some polynomial from n and M, should follow this. Many special cases of this problem are also NP-difficult. For example, the problem is NP-difficult in the strong sense at M = 1, $T_L = 0$, $\tau_{ij} = 0$, $d_h = 0$, $\alpha_h = 1$ and G = (N, $\emptyset$), and also at M = 1, $T_L = 0$, $\tau_{ij} > 0$, $d_h = \alpha_h = 0$ and G = (N, $\emptyset$) (the well-known traveling salesman problem is found in the latter case). Substantiation of the given results can be found in [2], where special cases of the considered problem are also determined, for which effective solving algorithms are known.

Specifically, an optimal schedule at $T_L=0$, $t_i=1$, $t_{ij}=\tau_{ij}=0$, $\alpha_h=0$ and G = = (N, $\emptyset$) can be constructed within $O(n \log_2 n)$ actions, while an optimal schedule can be constructed at $T_L=0$, $t_{ij}=\tau_{ij}=0$, $\alpha_h=0$ and upon authorization of interruptions in completing the operations can be constructed during $O(n^2)$ events.

The results of the postulated problem rather complexly predetermined the method of solving it. It is first solved by using a high-speed heuristic algorithm and an accurate algorithm of the branches and boundaries type is then used, in which the heuristic solution is used as the initial record.

4. The heuristic algorithm. The known procedure of constructing a schedule according to some list is realized [2].

Let a list P = $\{j_1, j_2, \ldots, j_h\}$ of parts of set X be compiled (the methods of compiling it are considered below). Let us describe a procedure for constructing schedule s according to this list.

1) Let us initially assume that $r = 1$, $l = 1$, $T'_L = T_L$, $L = \overline{1, M}$, $d'_h = d_h$, $h = \overline{1, k}$, where r is the ordinal number of the part in list P, l is the ordinal number of the operation on this part, T'_L is the current readiness time of the instrument L, and d'_h is the current readiness time of part h.

2) Let us find a device I = L, for which the minimum value is reached

$$\Delta_I = \begin{cases} T'_I, & \text{if } T'_J \geqslant d'_{j_r} \text{ at all } J = \overline{1, M}, \\ \max\{0,\ d'_{j_r} - T'_I\} & \text{otherwise.} \end{cases}$$

Let us designate fulfillment of operation $u = i^j_l$ by device L in schedule s and let us assume that the moment of its beginning $t^0_\mu(s)$ is equal to $\max\{T'_L, d'_{j_r}\}$. Let us assume that $T'_L = t^0_\mu(s) + \tau_{\nu\mu} + t_\mu$, where ν is the number of the last operation designated to device L. If no other operation is designated for device L, then $\tau_{\nu\mu} = 0$.

If some operations must still be performed on part j_r, i.e., $l \neq n(j_r)$, let us assume that $d'_{j_r} = T'_L + t_{\mu i^{j_r}_{l+1}}$, $l = l + 1$ and let us go on to step 2). If $l = n(j_r)$ and if $r < k$, we assume that $r = r + 1$, $l = 1$ and we turn to step 2). If $l = n(j_k)$, then all operations are distributed according to the devices an schedule s is constructed.

Different methods of compiling list P are possible. It is compiled by the following methods in the EVR program that implements the given algorithm. Parts $h \in X$ in list P are ordered either according to the nondecrease of parameter h, d_h or D_h or according to a nonincrease of parameter a_h or $t_h = \sum_{l=1}^{n(h)} t_{i^h_l} + \sum_{l=1}^{n(h)-1} t_{i^h_l i^h_{l+1}}$.

We note that assignment of operations to devices in the given procedure occurs essentially according to their list, which does not change during the calculations. One can suggest another approach in which the list is modified after each assignment of an operation to a device. This

approach presents greater opportunities to construct heuristic schedules, but implementation of it is more cumbersome.

One of the methods of formulating this "dynamic" list P is realized in the EVR program: the operations are ordered according to a nondecrease of the value $D_h - \bar{t}_i$, where i is an operation on part h and $\bar{t}_i$ is the moment of completion of operation i with assignment of it to device L, determined the same as in step 2) of the above procedure.

The result of operation of the EVR program is to which of the six constructed schedules the least value of specific function F(s) corresponds.

5. The exact algorithm. The basis of an algorithm of the branches and boundaries type is the following process of constructing a tree of the considered versions. It is formulated sequentially by levels, which are numbered from 0 to n, beginning with the root [2]. A set of all permissible schedules of the initial task corresponds to the root. The permissible (partial) schedule s_v of executing r operations from set N corresponds to each vertex v of level r, $1 \leq r < n$, organizational graph $G_v = (N_v, U_v)$, which determines the order of execution of the remaining n-r operations; the lower estimate (boundary) F_v of the value of the specific function on set Q_v of schedules obtained as a result of supplementing s_v to the (complete) permissible schedule.

Only vertices v, for which the value of F_v does not exceed the record $F(s^0)$, where s^0 is the best (record) of already constructed permissible schedules (since otherwise there is no schedule $s' \in Q_v$ such that $F(s') < F(s^0)$), belong to the branch. The value of F_v is calculated by the formula $F_v = F(s_v) + C$, where C is the optimal value of the specific function, found as a result of solving the initial problem on the assumption that $\check{N} = N_v$, $G = (\check{N}_v, \varnothing)$, $\check{t}_i = t = \min\limits_{j \in N_v} t_j + \min\limits_{i, j \in N_v} \tau_{ij}$, $\tau_{ij} = 0$, $i \in N$, $j \in N$, $\alpha_h = 0$, $h = \overline{1, k}$, and T_J is the moment of completion of the operation of device J, $J = \overline{1, M}$, upon schedule s_v. It is sufficient to perform $O(M(n - r))$ actions to solve this problem.

Some vertex of level r (vertex v for definiteness) is selected to formulate level r + 1 of the tree of variants. It is linked by edges to vertices $v_1, v_2, \ldots, v_q$ of the next (r + 1)-th level. Let us $N'(G_v)$ be a set of vertices of organizational graph G_v having no predecessors. Schedule s_{v_j}, $j = \overline{1, q}$, is found from schedule s_v as a result of assignment of some operation $i \in N'(G_v)$ to one of M devices. Organizational graph G_{v_j} is found from G_v as a result of removal of vertex i from G_v and removal of the arc (if such exists) that procedes from it. It is obvious that the value of q is equal to the number $M|N'(G_v)|$ of different assignments of operations to the devices.

The values of F_{v_j}, $j=\overline{1, q}$, are then calculated and if $F_{v_j} \geqslant F(s^0)$, vertex v_j is excluded from the tree of considered variants. If all vertices v_j, $j = \overline{1, q}$ are excluded, vertex v is also excluded. Another vertex of r-th level is then selected for formation of level r + 1.

The schedules s_{v_j} are completely permissible at r + 1 = n. In this case, $F_{v_j} = F(s_{v_j})$ and if $F_{v_j} < F(s^0)$, the record and the record schedule are replaced: $s^0 = s_{v_j}$, while vertex v_j is excluded from the tree of variants.

The process continues until the root of the tree of variants is excluded. The last record schedule will obviously be optimal.

Since the time complexity of the given algorithm is exponentially dependent on n and M, one can not always find a precise solution within an acceptable time. An ϵ-approximate solution [5] of the problem, i.e., a schedule s^ϵ at which $F(s^\epsilon) - F(s^*) \leqslant \varepsilon F(s^*)$, where $\epsilon \geq 0$ is any previously given number, is essentially constructed in the PLGAY program, which implements the given algorithm. Only those vertices v of the tree of variants for which $F_v(1+\varepsilon) < F(s^0)$, are considered, while the vertices v_j, for which $F_{v_j}(1+\varepsilon) \geqslant F(s^0)$, are excluded from the tree of variants. This ordinarily results in a considerable reduction of the number of considered variants.

6. Correction of schedules. A situation when a partially implemented schedule must be corrected, for example, with regard to the influx of unplanned applications, failure of equipment and so on, sometimes occurs during practical operation of the OKP system.

Let some parts machining schedule s of set X be partially realized. The operation of adjacent shops and sections, delivery of tools, complete set of blanks and so on is coordinated with the times of the beginning and end of machining the parts of set X upon schedule s. Let us assume that unplanned requests to machine some set of machine Y of new parts arrive at the section. The problem is to construct the machining schedule s′ of both new Y and old (but still not machined) parts $X' \subset X$ so that the deviation of the times of beginning and end of machining the parts of set X′ in schedule s′ from the corresponding moments in schedule s be minimal if possible. Disruption of this requirement may result in additional delays in subsequent coordination of the operating plans of the GAU other shops, sections and services.

The criterion of optimality, introduced in section 2, permits one to use the EVR and PLGAY programs to solve the postulated problem of schedule

correction. Let us assume for parts h $\in$ X, which have not yet arrived for machining, that $d_h=t_h^0(s)$, $D_h=\bar{t}_h(s)$ and let us increase the value of α_h considerably. Let us then solve the problem of constructing an heuristic or optimal schedule (depending on the time allocated for the calculations) of machining the parts of set X′ $\cup$ Y with regard to the modified values d_h, D_h and α_h, h $\in$ X′. This problem can be solved at different values α_h and one can select the best of the derived schedules.

This method of correcting the schedule guarantees with sufficient probability that deviations of the times of the beginning and end of machining the parts of set X′ from the corresponding moments in the old schedule s will be insignificant in the new schedule s′. The parts of set Y will be included in schedule s′ so as to minimize the value of F(s′). An experiment, conducted on real problems, showed that the given approach indeed yields good results of correcting the operating schedules of GAU.

7. Experience of appliation. The developed programs are found at the stage of experimental operation for machining GAU, which include two groups of machine tools (six IR-320 PMF4 machining centers and three IR-500 PMF4 machining centers), a SA-0.5 automated warehouse and the Elektronika NTsTM-25 transport robot. Each of the groups of machine tools has its own individual production plan and the schedules are compiled for each group separately.

The SM-1420.01 computer system is used as the OKP hardware. The operating system is the RV 3.0. The database management system is the MIRIS applications program package. The software for organizational-economic management of the GAU is represented schematically in the figure and comprises approximately 470 Kbytes. Approximately 65 Kbytes of this capacity is used by the optimal schedule construction programs, realized in Fortran-4 algorithmic language.

The total construction time of a near-optimal schedule (including reading the information for the database and output of tabulograms for 6 machine tools and 25 operations) comprises approximately 1 hour 15 minutes. The time of execution of the EVR program comprises approximately 1 min, while the time of execution of the PLGAY program fluctuates from several minutes to the maximum value established by the controller as a function of the given value of ϵ. Since finding a precise solution of the problem of compiling an optimal schedule requires rather large expenditures of computer time, the controller is ordinarily limited to finding an intermediate record schedule that guarantees the required load of the equipment.

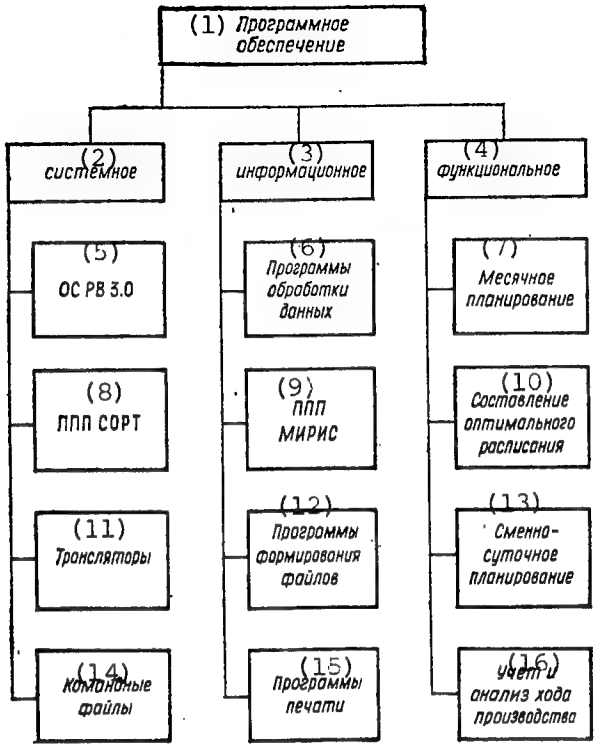

Software of Organizational-Economic Management of GAU

KEY:

1. Software
2. Systems
3. Database organization and management
4. Functional
5. RV 3.0 operating system
6. Data processing programs
7. Monthly planning
8. SORT applications program package
9. MIRIS applications program package
10. Compilation of optimal schedule
11. Translators
12. File-forming programs
13. Shift-daily planning
14. Command files
15. Print programs
16. Accounting and analysis of course of production

An economic impact totalling 22,400 rubles was found for the more optimal distribution and ordering of operations at the GAU. The average operating time was reduced by 10-12 percent and the equipment load was increased by approximately 10 percent.

BIBLIOGRAPHY

1. Chudakov, A. D. and B. Ya. Falevich, "Avtomatizirovannoye operativno-kalendarnoye planirovaniye v gibkikh kompleksakh mekhanoobrabotki" [Automated Operational-Calendar Planning in Flexible Machining Systems], Moscow, 1986.

2. Tanayev, V. S., V. S. Gordon, and Ya. M. Shafranskiy, "Teoriya raspisaniy. Odnostadiynyye sistemy" [Scheduling Theory. One-Stage Systems], Moscow, 1984.

3. Garry, M. and D. Johnson, "Vychislitelnyye mashiny i trudnoreshayemyye zadachi" [Computers and Difficultly-Resolvable Problems], Msocow, 1982.

4. Sotskov, Yu. N. and V. B. Alyushkevich, DOKLADY AKADEMII NAUK BSSR, Vol 32, No 2, 1988.

5. Kovalev, M. Ya. and Ya. M. Shafranskiy, ZhVM i MF, No 7, 1986.

UDC 629.124.791:620.193

Study of Effectiveness of Ice-Resistant Coatings in Protection of Icebreaker Hulls

907F0182A Leningrad SUDOSTROYENIYE in Russian No 12, Dec 89 pp 33-36

[Article by V. A. Babtsev and G. P. Shemendyuk]

[Text] Coatings that permit protection of the hull of icebreakers and ships that navigate in ice against corrosion and abrasive wear have been used ever more extensively during the past few years. They include epoxide-based paints Inerta-160 of the Finnish Technos-Winter Company and of type Permax with glass flakes of the Japanese Chugoku Marine Paints Company, Zabron Polyurethane Coating of the Xenex Company (United States) and some others.

The main advantage of these coatings is their durability, which permits an increase of the period between dry dock; the coatings provide rather reliable protection of plates and weld seams of the plating against wear upon friction against ice. Examples of their use are shown in Figures 1-3. A coating of the Permax type showed good wear resistance: it was retained on an area of approximately 80-85 percent after 2 years of operation in ice (four navigation seasons). The low frictional coefficient of the coatings against ice reduces the ice resistance of the hull, increasing the ice trafficability of the ship and contributing to conservation of fuel.

It is important to estimate the effectiveness of using ice-resistant coatings from the viewpoint of reducing metal expenditures in construction of ships and during subsequent repair.

The margin of a plate without protective coating for wear, as is known, is created by increasing the thicknesses of the plates compared to the permissible residual thicknesses that guarantee safe operation of the icebreaker between inspections.

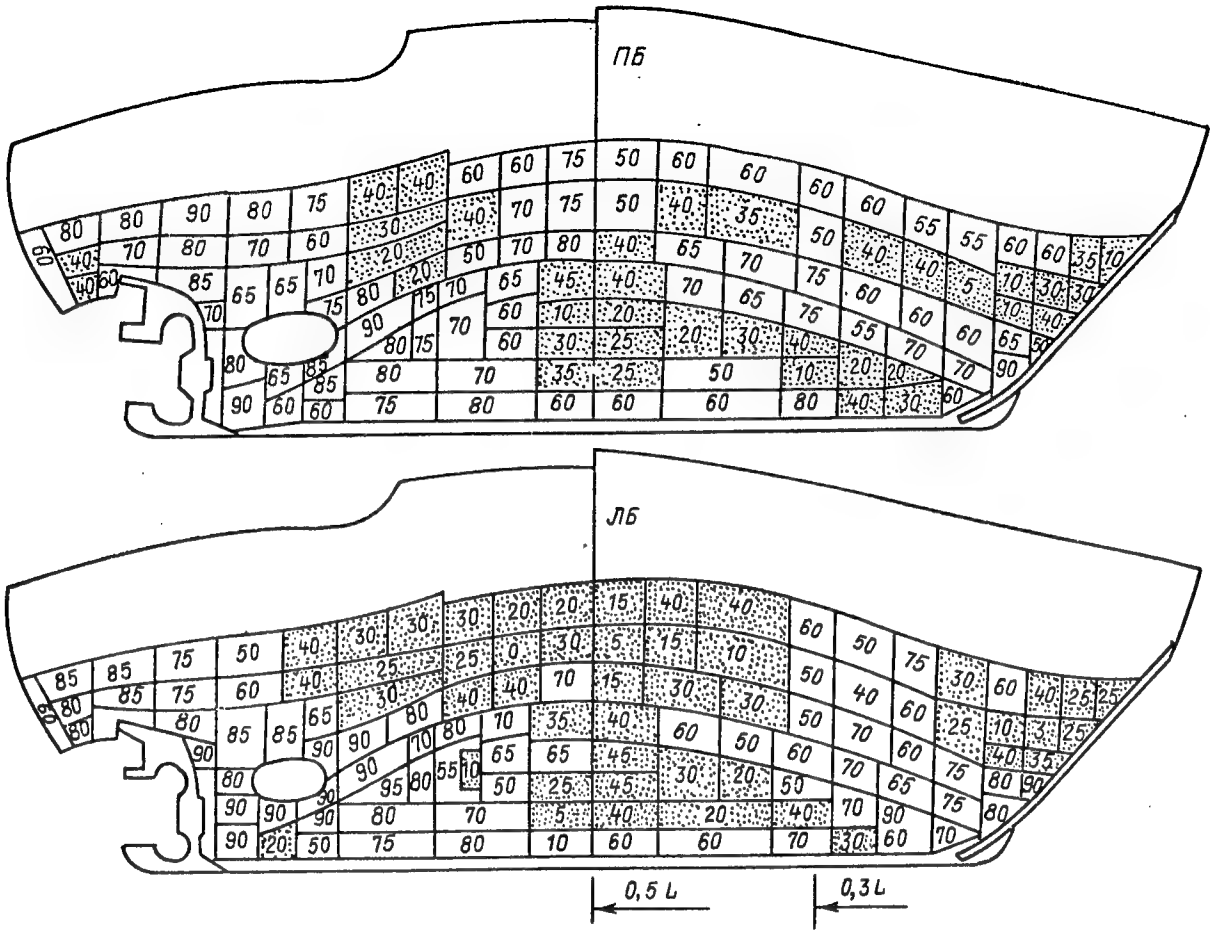

Figure 1. Degree of Retention of Inerta-160 Ice-Resistant Coating (Applied During Repair) After 3 Years of Operation of the Icebreaker "Kapitan Khlebnikov".
The numbers denote the residual area of the coating within the plate, percent. Plates on which less than 50 percent of the coating is retained are denoted by points

The permissible standards of wear of the plate for different regions of the hull were obtained on the basis of statistical rates of wear for icebreakers with different categories of ice reinforcement of the hull (data for category LL2 are presented in Table 1) and with different loads, determined by the residual deflections of the plate. These standards are presented in Table 2 in the form of coefficients n_1 and n_3, contained in formula (1). (Footnote) (The permissible thicknesses $[s_1]$ and $[s_3]$, on the basis of which values n_1 and n_3 were found, were calculated with the participation of postgraduate student O. I. Bratukhin)

The permissible residual thicknesses s_1 and s_3, by analogy with the standard methodical instructions of the USSR Registry on evaluation of the technical state of operated ships, can be calculated by the formulas

$$[s_1] = n_1(s_c - c); \quad [s_3] = n_3(s_c - c), \tag{1}$$

where s_c is the construction thickness, required by the Regulations of the USSR Registry for a specific region of the hull, c is the allowance for wear by the same regulations, and n_1 and n_3 are the recommended standard coefficients for total and local wear with regard to the arrangement of the plates by length and width (height) of the hull and according to the category of icebreakers (see Table 2).

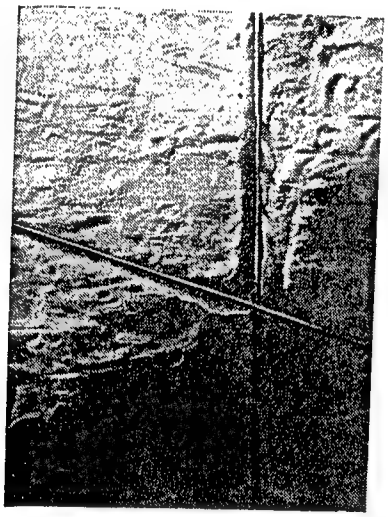

Figure 2. Corrosion Breakdown at Points of No Inerta-160 Coating on Icebreaker "Kapitan Khlebnikov," Specifically in the Zone of Thermal Influence Along Weld Seams.
Depth of pits--up to 1.0-1.5 mm

The wear margin on a plate protected by a coating in some region (ij) is expended at the rate v_{ij} during time t_p, that is,

$$s_{c_{ij}} - [s_{ij}] = v_{ij} t_p^{\gamma}, \tag{2}$$

where γ is the statistical factor found from the results of data processing on the rates of wear and v_{ij} is the rate of wear (reduction

of thickness) in the region of the hull. The subscripts denote: i is the region along the length of the hull, and j is the region along the strake. The subscripts are subsequently omitted.

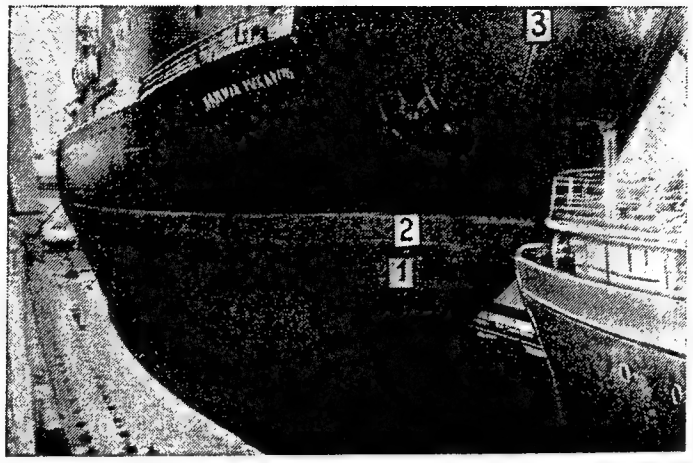

Figure 3. Wear of Icebreaker Coatings on Icebreaker "Admiral Makarov" (Applied During Repair): 1--Permax 3000 coating (thickness of exposed lower white layer is equal to half of total thickness of coating); 2--Zebron coating (width of section of this coating is equal to width of plates of ice strake; greatest wear near stem); 3--upper boundary of wear of plate from icebreaker

The service life of some region of the hull will then be equal to

$$t_p = \sqrt[\gamma]{\frac{s_c - [s]}{v}}. \tag{3}$$

Using the method of linearization [1], one can find the mean value t_p and the mean square deviation s_{t_p} by the formulas

$$\bar{t}_p = \left(\frac{s_c - [s]}{\bar{v}}\right)^{1/\gamma}; \tag{4}$$

$$s_{t_p} = \sqrt{D_{t_p}}; \quad D_{t_p} = \left[\frac{\sqrt[\gamma]{s_c - [s]}}{\gamma \bar{v}^{(1+\gamma)/\gamma}}\right]^2 Dv, \tag{5}$$

where $\bar{v}$, D_v and γ are assumed known as a result of statistical processing of data about wear.

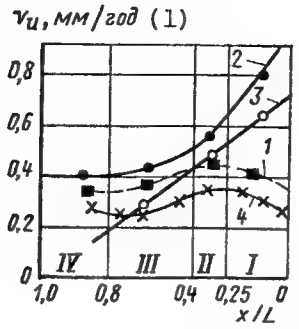

Figure 4. Distribution of Mean Rates of Wear of Outer Plate of Icebreaker: 1--ice strake; 2--bilge; 3--flat part of bottom (1, 2 and 3 are related to icebreaker of category LL3); 4--ice strake of icebreaker of category LL1. Regions of hull: I--bow; II--intermediate; III--middle; IV--stern

KEY:

1. mm/year

Table 1. Rates of Wear of Plating of Icebreaker "Moskva," mm/Year (Main Value--Mean Square Deviation--Coefficient of Variation, Respectively)

(1) Район корпуса		(2) Скуловая часть			(3) Плоская часть днища		
Носовой	(4)	0,81	0,333	0,411	0,60	0,422	0,703
Промежуточный	(5)	0,56	0,239	0,427	0,46	0,27	0,586
Средний	(6)	0,43	0,206	0,479	0,28	0,17	0,607
Кормовой	(7)	0,40	0,257	0,640	—	—	—

KEY:

1. Region of hull
2. Bilge part
3. Flat part of bottom
4. Bow
5. Intermediate
6. Middle
7. Stern

Table 2. Standard Coefficients of Wear m_1 and n_3 for Plating of Icebreakers

(1) Район корпуса	(2) Ледовая категория	(3) Ледовый пояс		Скуловая часть (4)		Плоская часть (5)	
		n_1	n_3	n_1	n_3	n_1	n_3
(6) Носовой	(7) ЛЛ1	0,83	0,73	0,79	0,73	См. примечание (8)	
	ЛЛ2	0,78	0,69	0,72	0,65		
	ЛЛ3	0,73	0,65	0,65	0,63		
	ЛЛ4	0,68	0,65	0,58	0,61		
(9) Промежуточный	ЛЛ1	0,81	0,65	0,76	0,62	0,75	0,62
	ЛЛ2	0,76	0,63	0,70	0,60	0,68	0,58
	ЛЛ3	0,71	0,61	0,62	0,58	0,60	0,53
	ЛЛ4	0,66	0,59	0,55	0,56	0,52	0,48
(10) Средний	ЛЛ1	0,79	0,63	0,69	0,61	0,65	0,58
	ЛЛ2	0,75	0,61	0,64	0,59	0,60	0,54
	ЛЛ3	0,70	0,59	0,60	0,57	0,55	0,50
	ЛЛ4	0,65	0,57	0,54	0,56	0,50	0,46
(11) Кормовой	ЛЛ1	0,76	0,63	0,60	0,55	См. примечание (8)	
	ЛЛ2	0,72	0,60	0,60	0,55		
	ЛЛ3	0,68	0,56	0,60	0,50		
	ЛЛ4	0,65	0,53	0,60	0,50		

Note. If flat bottom is present in bow and stern regions, n_1 and n_3 are then equal to corresponding values of coefficients for bilge.

KEY:

1. Region of hull
2. Ice category
3. Ice strake
4. Bilge part
5. Flat part
6. Bow
7. LL
8. See note
9. Intermediate
10. Middle
11. Stern

The results of statistical processing of data on the rates of wear of one of the regions of the ice strake of an icebreaker of category LL1 are presented in Figure 5.

If one assumes that the mean times between failures t_p is distributed according to truncated normal law [1, 2], the probability of trouble-free operation of plating not protected by a coating is determined according to the wear condition by the function

$$P(t_p) = \frac{1}{2}\left[1 - \Phi\left(\frac{t_p - \bar{t}_p}{\sqrt{2}\, s^2_{t_p}}\right)\right], \qquad (6)$$

where Φ is a Laplace function.

One can determine the number of sheets that must be replaced for region ij containing N sheets of plating, having identical rate of wear, by the following formula:

$$n_{ij} = [1 - P(t_p)]\, N_{ij}. \qquad (7)$$

The number of sheets that require replacement within the next time interval t'_p will be equal to

$$n'_{ij} = (N_{ij} - n_{ij})\left[1 - P\left(t'_p\right)\right] \text{ and so on.} \qquad (8)$$

The volume of replacements can be calculated at interval of 2-4 years to the end of the service life of the ship, assuming that the thicknesses of the sheets did not change during the adopted time interval.

Using the derived probability of failure due to wear, one can determine the γ-percent service life, i.e., the service life of the plating to repair with given probability [3]

$$T_\gamma = T_{cp}(1 - V_x U_\gamma),$$

where U_γ is the quantile of normal distribution at given γ-percent service life and V_x is the variation coefficient. The use of simulation models is more promising.

Knowing the number of sheets that require replacement, their thickness, the volume of the accompanying jobs, and the cost of the material, one can determine the expenditures for repair for the entire operating period [4]

$$З_p = \sum_{t=1}^{t_p} \frac{И}{(1+E)^{t_p}} + \frac{З_p^{t_{p_1}}}{(1+E)^{t_{p_1}}} + \frac{З_p^{t_{p_2}}}{(1+E)^{t_{p_1}}} + \cdots,$$

where E is a standard coefficient (0.1), И is the operating expenses (dry docking, survey of defects, cleaning, application of ordinary paint and so on), and 3^{t}_{p} are the expenditures for manufacture of the replaced structure.

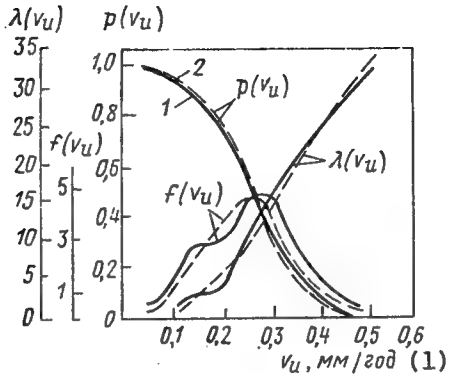

Figure 5. Real (1) and Calculated (2) Normal Probability Distribution $p(v_{н})$, Probability Density $f(v_{н})$ and Distribution Intensity $\lambda(v_{н})$ of Wear of Plating ($v_{н}$) of Ice Strake in Middle Part of Hull of Icebreaker of Category LL1

KEY:

1. mm/year

The expression in the numerator reduces the expenditures according to the time factor to the beginning of operation. The values of 3^{t}_{p} should be expressed by the design parameters--the thickness of the plating and the structural characteristics of the framing.

Using experiment planning theory, one can find the regression formulas that link the cost of manufacture of 1 ton of considered structure to its parameters. For example, the function for the flat bottom floor of an icebreaker of category LL3 has the form (rubles/t)

$$Ц = 7820 + 80s_{н.о} - 55s_{о.н} + 132s_{р.н} + 14s_{н.о}s_{р.н},$$

where $s_{н.о}$, $s_{о.н}$, and $s_{р.н}$ are the thicknesses of the outer plating, main framing and framing, mm. Only half the height of the structure, ordinarily replaced during repair, is taken into account.

Adding $З_р$ and Ц, we find a specific function, which can be used to determine the optimal thicknesses of the outer plating, corresponding to the optimal metal expenditures (Figure 6).

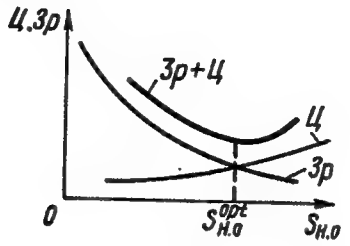

Figure 6. Minimization of Total Expenditures for Repair ($З_р$) and Manufacture (Ц) of Floor as Function of Thickness of Plating

Similar estimates of the expenditures can also be made for ice-resistant coatings. For example, for plating protected by ice-resistant coating, the service life has the form

$$t_р = \sqrt[1]{s_п/v_п},$$

where $s_п$ is the thickness of the coating and $v_п$ is the rate of wear of the coating (decrease of its thickness).

Measurements of the residual thicknesses of ice-resistant Permax 3000 epoxide coating showed that the average rate of wear in the bow region was equal to 0.34 mm/year. The results of measuring the residual thicknesses of the coating on sections of the ice strake and bilge of an icebreaker are presented in Figure 7. Operating experience and examination of Permax 3000, Inerta-160 and Zebron coatings showed their high resistance upon friction against ice. Using the above formulas, one can find the expenditures $З_р$ for restoration of the ice-resistant coating.

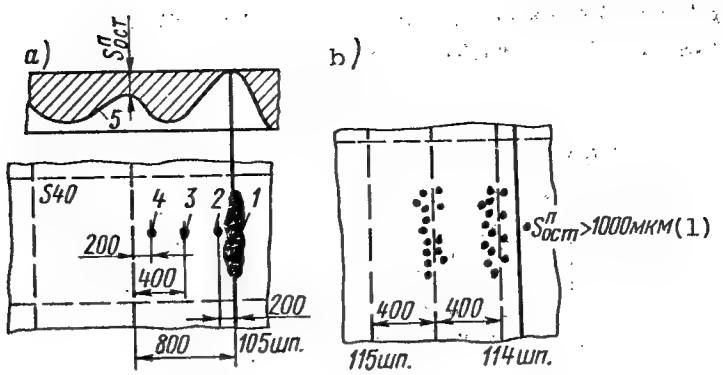

Figure 7. Wear of Permax 3000 Ice-Resistant Coating After 2 Years of Operation of Icebreaker of Category LL2 (Since 1984) on Sections of Bilge (a) and Ice Strake (b):

a--residual thickness of coating $S^{п}_{ост}$ at point of 1-0 μm; 2--540 μm; 3--1,000 μm; 4--1,100 μm; 5--nature of wear of coating between framing; b--$S^{п}_{ост}$ is average of 665 μm and minimum of 500 μm. Initial thickness of coating is 1,100-1,400 μm

KEY:

1. μm

However, breakdown of the coating by cracking in regions of intensive deformations is observed in practice (Figure 8). Testing of specimens with Inerta-160 coating, applied to a dry-sanded surface of steel with complete observation of the recommended technology, showed that the strength of the layer of coating is dependent on its thickness (Figure 9). Taking this into account, one should proceed when designating the thickness of the coating not only from wear durability, increasing the thickness of the layer at points of intensive ice loads, but one should also take into account the probability of cracking of thick layers of the coating at points of the greatest deformations of the sheets of plating (near the framing). After cracks form, the process of further breakdown occurs more intensively as a result of corrosion of the metal due to penetration of sea water along the cracks. Corrosion furrows then form on the surface of the plating along the support contour of the plates, which naturally contributes to a reduction of the strength of the plating.

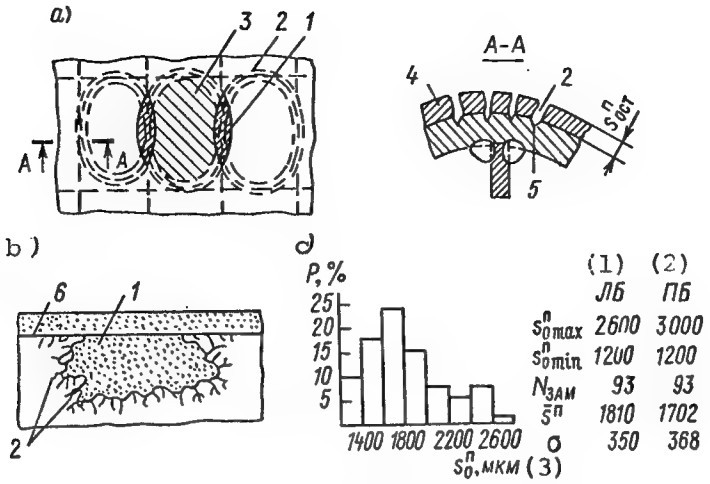

Figure 8. Breakdown of Permax 3000 Ice-Resistant Coating in Bilge Part (a) and of Zebron Coating on Ice Strake (b) of Icebreaker of Category LL2; c--Statistical Data on Distribution of Initial Thicknesses $S^{П}_{0}$ of Zebron Coating on Ice Strake (1984): 1--absence of coating; 2--cracks in coating; 3--residual deflection of plating; 4--coating; 5--corrosion breakdown of steel; 6--upper edge of Zebron coating on ice strake

KEY:

1. Port
2. Starboard
3. μm

The probability of trouble-free operation according to the condition of deformation stability of the coating can be written in the form

$$R = P\left([\varepsilon^{п}] > \varepsilon_{пл}\right),$$

where $[\epsilon^{П}]$ is the permissible deformation of the coating upon tension and $\epsilon_{ПЛ}$ is the deformation on the surface of the plate during bending and tension.

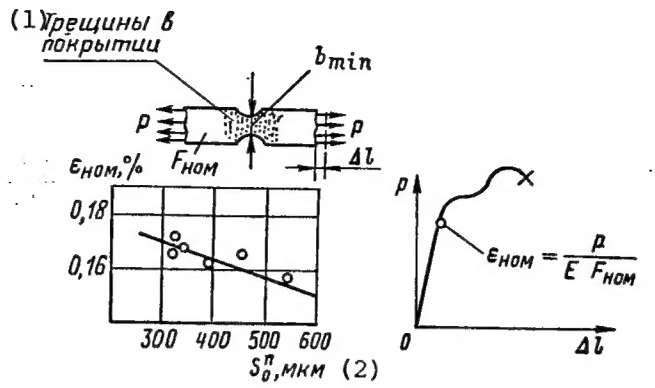

Figure 9. Appearance of Cracks in Layer of Inerta-160 Coating Upon Deformation of Specimens With Different Thickness of Coating

KEY:

1. Cracks in coating
2. μm

The value of R for the coating has much in common with the characteristics of fatigue failures of metal and the corresponding approach can be used to determine it. The number of loading cycles is equal to the number of impacts of small pieces of ice, present in the considered region (Figure 10). All the values necessary for calculation can be found only experimentally [5]. Multiplying the probability of failure due to wear by the probability of failure due to cracking or separation of the coating from the metal, we find the resulting probability of failure, for which one can find the expenditures to restore the coating during the operating period of the ship. Optimizing according to the thickness of the metal and comparing the opltimal thicknesses of a protected and unprotected plating, one can estimate the saving due to reduction of metal expenditures as a result of using an ice-resistant coating (while naturally retaining the necessary strength of the structures).

Preliminary estimates according to the given method and the experience of operating ships with ice-resistant coatings permit some practical conclusions:

1. One must know the parameters of wear resistance and the deformation capacity of the coatings, their fatigue life when exposed to variable loads, and also the laws of distribution of the loads for regions of the hull for more complete estimation of the effectiveness of ice-resistant coatings of the hull of icebreakers or ships that navigate in ice that are well recommended.

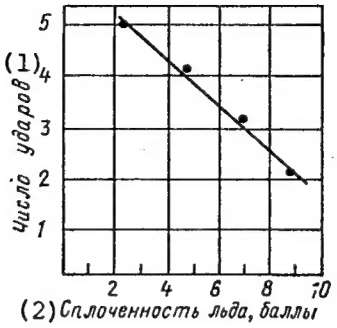

Figure 10. Number of Impacts of Small Pieces of Ice on Section of Plating 10 m^2 in Area and of Bow Transition Regions of Bottom of Icebreaker of Category LL3 During 1 Hour of Running Time for Each Knot of Speed (From Experimental Data)

KEY:

1. Number of impacts
2. Density of ice, units

2. The use of ice-resistant coatings in regions of the hull with large spacing and relatively small thicknesses of the sheets of plating may be unfeasible. The effectiveness of using ice-resistant coatings for icebreakers has now been confirmed if the ratio of the length of the least support side of the plate to its thickness is less than or equal to 26. It is recommended that ice-resistant coatings be applied 2-3 mm thick in the bow and intermediate regions along the entire height of the underwater part of the hull, 1.5-2 mm thick in the middle and stern regions of the ice strake, and 1.0-1.5 mm thick on the bilge and flat part of the bottom on Arctic icebreakers of categories LL1-LL2. The corresponding values can be reduced by 25 percent for icebreakers of category LL3 and by 35-40 percent for icebreakers of category LL4 and ULA [not further identified] ships.

BIBLIOGRAPHY

1. Ventsel, Ye. S. and L. A. Ovcharov, "Prikladnyye zadachi teorii veroyatnostey" [Applied Problems of Probability Theory], Moscow, Izdatelstvo "Vysshaya shkola", 1979.

2. Yekimov, V. V., "Nadezhnost konstruktsiy s uchetom sluchaynykh faktorov. Uchebnoye posobiye" [The Reliability of Structures With Regard to Random Factors. A Textbook], Leningrad, LKI, 1975.

3. Yefremov, L. V., "Praktika inzhenernogo analiza nadezhnosti sudovoy tekhniki" [The Practice of Engineering Analysis of the Reliability of Ship Equipment], Leningrad, Izdatelstvo "Sudostroyeniye", 1980.

4. Lyubushin, N. A., "Ekonomicheskaya effektivnost proyektnykh resheniy v sudokorpusostroyenii" [The Economic Impact of Design Solutions in Ship Hull Building], Leningrad, Izdatelstvo "Sudostroyeniye", 1982.

5. Barabanov, N. V., V. A. Babtsev, and N. A. Ivanov, "Ice Loads on Bottom Structures of Ships," SUDOSTROYENIYE, No 11, 1982.

- END -

10

22161
37

NTIS
ATTN: PROCESS 103
5285 PORT ROYAL RD
SPRINGFIELD, VA 22161

Foreign Broadcast Information Service (FBIS) and Joint Publications Research Service (JPRS) publications contain political, economic, military, and sociological news, commentary, and other information, as well as scientific and technical data and reports. All information has been obtained from foreign radio and television broadcasts, news agency transmissions, newspapers, books, and periodicals. Items generally are processed from the first or best available source; it should not be inferred that they have been disseminated only in the medium, in the language, or to the area indicated. Items from foreign language sources are translated; those from English-language sources are transcribed, with personal and place names rendered in accordance with FBIS transliteration style.

Headlines, editorial reports, and material enclosed in brackets [ ] are supplied by FBIS/JPRS. Processing indicators such as [Text] or [Excerpts] in the first line of each item indicate how the information was processed from the original. Unfamiliar names rendered phonetically are enclosed in parentheses. Words or names preceded by a question mark and enclosed in parentheses were not clear from the original source but have been supplied as appropriate to the context. Other unattributed parenthetical notes within the body of an item originate with the source. Times within items are as given by the source. Passages in boldface or italics are as published.

SUBSCRIPTION/PROCUREMENT INFORMATION

The FBIS DAILY REPORT contains current news and information and is published Monday through Friday in eight volumes: China, East Europe, Soviet Union, East Asia, Near East & South Asia, Sub-Saharan Africa, Latin America, and West Europe. Supplements to the DAILY REPORTs may also be available periodically and will be distributed to regular DAILY REPORT subscribers. JPRS publications, which include approximately 50 regional, worldwide, and topical reports, generally contain less time-sensitive information and are published periodically.

Current DAILY REPORTs and JPRS publications are listed in *Government Reports Announcements* issued semimonthly by the National Technical Information Service (NTIS), 5285 Port Royal Road, Springfield, Virginia 22161 and the *Monthly Catalog of U.S. Government Publications* issued by the Superintendent of Documents, U.S. Government Printing Office, Washington, D.C. 20402.

The public may subscribe to either hardcover or microfiche versions of the DAILY REPORTs and JPRS publications through NTIS at the above address or by calling (703) 487-4630. Subscription rates will be provided by NTIS upon request. Subscriptions are available outside the United States from NTIS or appointed foreign dealers. New subscribers should expect a 30-day delay in receipt of the first issue.

U.S. Government offices may obtain subscriptions to the DAILY REPORTs or JPRS publications (hardcover or microfiche) at no charge through their sponsoring organizations. For additional information or assistance, call FBIS, (202) 338-6735,or write to P.O. Box 2604, Washington, D.C. 20013. Department of Defense consumers are required to submit requests through appropriate command validation channels to DIA, RTS-2C, Washington, D.C. 20301. (Telephone: (202) 373-3771, Autovon: 243-3771.)

Back issues or single copies of the DAILY REPORTs and JPRS publications are not available. Both the DAILY REPORTs and the JPRS publications are on file for public reference at the Library of Congress and at many Federal Depository Libraries. Reference copies may also be seen at many public and university libraries throughout the United States.